

Experimental and DFT study on pyrrole tosylhydrazones

R.N. Singh*, Poonam Rawat, Divya Verma, Shailendra Kumar Bharti

Department of Chemistry, University of Lucknow, Lucknow 226007, UP, India



HIGHLIGHTS

- FT-IR spectra of PT and EDTEPC were recorded and compared with the theoretical results.
- The feasibility of the reaction has been checked with the help of electronic descriptors.
- The calculated first hyperpolarizability ($\beta_0 = 6.50/8.38 \times 10^{-30}$) of PT and EDTEPC.
- Electronic transitions and chemical shifts have been also calculated.

ARTICLE INFO

Article history:

Received 14 August 2014

Received in revised form 19 October 2014

Accepted 20 October 2014

Available online 1 November 2014

Keywords:

B3LYP

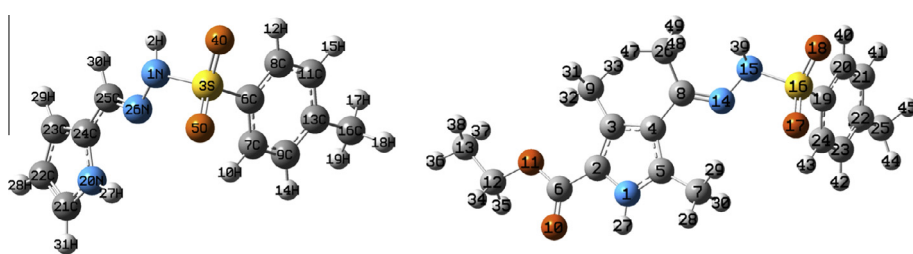
FT-IR

Red shift

Dimer

First hyperpolarizability

GRAPHICAL ABSTRACT



ABSTRACT

Two pyrrole tosylhydrazones, *1H*-pyrrole-2-tosylhydrazone (PT) and ethyl 3,5-dimethyl-4-(1-(2-tosylhydrazone)ethyl)-*1H*-pyrrole-2-carboxylate (EDTEPC) have been synthesized and characterized by various spectroscopic techniques. All calculations have been performed using B3LYP functional and 6-31G(d,p) basis set. The result of hydrogen bonding is obvious in ¹H NMR and FT-IR due to down field chemical shift and vibrational red shift to pyrrole N—H proton, respectively. The red shift in both the proton donor (pyrrole N—H) and proton acceptor (S=O) group designates presence of intermolecular classical hydrogen bonding N—H···O. The binding energy of dimer formation is calculated as 13.12, 14.12 kcal/mol, after correction in basis set superposition error (BSSE). Topological parameters indicate the weaker interactions presents in the molecules. The global electrophilicity index ($\omega = 2.54, 2.28$ eV) shows that PT and EDTEPC molecules are strong electrophile. The local reactivity descriptors analyses are performed to determine the reactive sites within the PT and EDTEPC. Computed first hyperpolarizability ($\beta_0 = 6.50/8.38 \times 10^{-30}$ esu) of PT and EDTEPC indicates non-linear optical (NLO) response of the molecules.

© 2014 Elsevier B.V. All rights reserved.

Introduction

Hydrazones have triatomic >C=N—N< linkage, containing two connected nitrogen atoms of different nature and a C=N double bond that is conjugated with a lone electron pair of the terminal nitrogen atom. These structural fragments are mainly responsible for the physical and chemical properties of hydrazones [1]. Hydrazones possess an azomethine proton —CH=N—NH— and constitute an important class of compounds for different types of biological activity such as antibacterial [2,3], antidepressant [4],

anti-inflammatory, analgesic [5,6] and anti-pyretic [7–9]. They are versatile starting materials for the synthesis of a variety of N, O or S containing heterocyclic compounds such as oxadiazolines, thiazolidinones, triazolines, and various types of other organic compounds [10–21].

Sulfonylhydrazide and sulfonylsemicarbazide derivatives exhibit a variety of bacteriostatic activity and also are important compounds as blowing agents in cellular rubber and plastics. The aromatic sulfonylhydrazides are particularly useful in the production of azo dyes [22]. Due to the presence of a sulfonamide proton (—NH—SO₂—) these compounds have strong coordinating ability towards metal ions [23]. As per literature survey synthesis and brief spectral analysis of *1H*-pyrrole-2-tosylhydrazone was reported by Richard et al. in 1978 [24].

* Corresponding author. Tel.: +91 9451308205.

E-mail address: rnsvk.chemistry@gmail.com (R.N. Singh).

Hydrogen bonds are also of versatile importance in fields of chemistry and bio-chemistry, which governs chemical reactions, supramolecular structures, molecular assemblies and life processes. The quantum chemical calculation is powerful approach for study of different aspects of compounds [25,26].

In view of various significance of Pyrrole sulfonylhydrazone, ethyl 3,5-dimethyl-4-(1-(2-tosylhydrazone)ethyl)-1*H*-pyrrole-2-carboxylate (EDTEPC) has been synthesized. In this paper we present the structural, spectral and quantum chemical study of both PT and EDTEPC. The present investigation reveals the detailed spectroscopic nature of PT and EDTEPC and contributes to the understanding of the FT-IR spectra that these compounds contain hydrogen bonding. With the help of Bader's theory of "Atoms in molecules" (AIM) nature and strength of bonding have been revealed [27]. The theory of AIM efficiently describes H-bonding and its concept without border. Information about the potential energy distribution (PED) over the internal coordinates, conformations of the molecule together with complete analysis of geometry and chemical reactivity help in understanding the structural and spectral characteristics, have been studied. In particular, the interest in these compound provides opportunity for synthesis of new heterocyclic compounds, metal and organometallic complexes that may have considerable pharmacological activities and material applications. Therefore, the PT and EDTEPC was synthesized and characterized. In this paper we report the synthesis, detailed molecular structure, spectroscopic analysis and chemical reactivity of PT and EDTEPC using experimental and quantum chemical calculations.

Experimental details and quantum chemical calculations

The Mass spectrum of PT and EDTEPC were recorded on JEOL-Acc TDF JMS-T100LC, Accu TOF mass spectrometer. The ¹H NMR spectra of PT and EDTEPC were recorded in DMSO-d₆ on Bruker DRX-300 spectrometer using TMS as an internal reference. The FT-IR-spectra of PT and EDTEPC were recorded in KBr medium on a Bruker-spectrometer. The UV-Visible absorption spectra of PT and EDTEPC, (1×10^{-5} M in DMSO) were recorded on ELICO SL-164 spectrophotometer. All the quantum chemical calculations have been carried out with Gaussian 09 program package [28] to predict the molecular structure, energies of the optimized geometry, ¹H NMR chemical shifts and vibrational wavenumbers using DFT level of theory, B3LYP functional and 6-31G(d,p) as basis set. The optimized geometrical parameters are used in the vibrational wavenumbers calculation to characterize all stationary points as minima and their harmonic vibrational wavenumbers are positive. Potential energy distribution (PED) along internal coordinates is calculated by Gar2ped software [29]. Molecular graph were computed using AIMALL software [30]. To estimate the enthalpy (H) and Gibbs free energy (G) values, thermal corrections to the enthalpy and Gibbs free energy are added to the calculated total energies.

Preparation of 1*H*-pyrrole-2-tosylhydrazone (PT)

A solution of 4-methylbenzenesulfonylhydrazide (0.2134 g, 1.1464 mmol) in 15 ml methanol and 0.01 ml of conc. HCl as catalyst was added drop-wise with stirring in solution of 2-formyl-1*H*-pyrrole (0.250 g, 1.1464 mmol) in 10 ml methanol at room temperature. After stirring for 12 h, the precipitate was obtained. The precipitate was filtered by vacuum filtration, washed with methanol and dried in air, afforded (0.200 g, 45.17%) of PT, as orange color solid. m.p. 169–173 °C; Anal. calcd. for C₁₂H₁₃N₃O₂S: C 54.74%, H 4.98%, N 15.96%, obs.: C 54.02%, H 4.72%, N 15.44%. MS (m/z): calcd. 263.07, obs. 264 [M+H]⁺.

Synthesis of ethyl 3,5-dimethyl-4-(1-(2-tosylhydrazone)ethyl)-1*H*-pyrrole-2-carboxylate (EDTEPC)

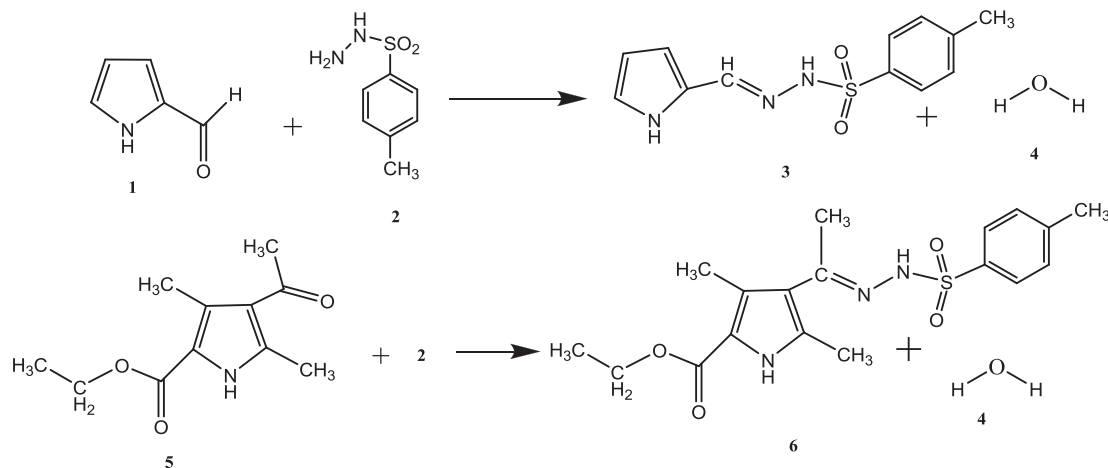
The solution of ethyl 4-acetyl-3,5-dimethyl-1*H*-pyrrole-2-carboxylate [26] (0.200 g, 0.9564 mmol) in 20 ml methanol was added dropwise to a stirred solution of para-toluene sulphonyl-hydrazide (0.1779 g, 0.9564 mmol) dissolved in 20 ml methanol. Two drops of polyphosphoric acid were added as a catalyst. Reaction mixture was refluxed for 36 h. A white color precipitate appeared. The precipitate was filtered off, washed with methanol and dried in air. Yield: 65% Color: white, m.p. 210 °C; Anal. calcd. for C₁₇H₂₁N₃O₄S: C 56.18%, H 5.82%, N 11.56%, obs.: C 56.02%, H 5.72%, N 11.44%. MS (m/z): calcd. 363.43, obs.: 364 [M+H]⁺.

Results and discussion

Molecular structures, dimerization and Quantum Theory of Atoms in Molecules (QTAIM) analysis

Scheme 1 shows the formation of PT and EDTEPC compound. Selected optimized geometrical parameters of PT and EDTEPC, calculated at B3LYP/6-31G(d,p) are listed in Supplementary Table S1a and Table S1b. The optimized geometries of PT and EDTEPC are shown in **Fig. 1**. The studied molecules possess C₁ symmetry. In both of the studied compounds tosylhydrazonemethyl group in PT and EDTEPC are away from the plain by N26—N1—S3—C6, N14—N15—S16—C19 torsion angle of 59.93°, 77.55° respectively. The conformation of the N—N—S—O linkage is *anti*, with torsion angles of 169.21°, -37.77°, which giving a folded appearance in both PT and EDTEPC molecules, respectively. The asymmetry of N—C bonds in the pyrrole has been observed in EDTEPC molecule due to the presence of the ethoxy group present at C2 of pyrrole ring. The molecular structure of PT and EDTEPC shows E-configuration of the hydrazone double bond. The presence of a methylene and sulphonamide frame between the pyrrole and benzene moieties allows the benzene ring and the pyrrole system to be somewhat parallel with respect to each other, so that the molecule adopts a U-shaped spatial conformation. The crystal structures of synthesized compounds have not been reported but geometrical parameters are taken for optimization from the crystal structure of 4-ethyl benzene sulfonylhydrazones [31]. Optimized geometry for monomer and dimer of PT and EDTEPC are shown in **Fig. 2**, respectively. Both molecules exist in the form of dimer. The dimer of EDTEPC form eight member ring, due to the intermolecular classical hydrogen bonding (N—H···O) both proton donor (N—H bond) and proton acceptor (C=O bond) are elongated by 1.0204 from 1.0103 Å(monomer) and 1.232 from 1.224 Å(monomer), respectively. EDTEPC also form dimer through hydrazone N—H and S=O group. The dimer of EDTEPC through hydrazone N—H and S=O group is higher in energy than EDTEPC dimer through N—H and C=O group. Total energy for ground state lower energy dimer of EDTEPC is calculated as -3126.18000 a.u. The PT forms dimer through hydrazone N—H and S=O group. The total energy of PT is calculated as -2355.84276 a.u. The elongation of 1.0314 Å (1.0234 Å monomer), 1.464 Å (1.478 Å monomer) in bond length of hydrazone N—H and tosyl S=O group, respectively, in PT dimer. The calculated binding energy of EDTEPC and PT dimer formation are found as 13.12, 14.12 kcal/mol, respectively, after correction in basis set superposition error (BSSE) via standard counterpoise method [32].

The calculated thermodynamic parameters for dimerization reaction at 25 °C are listed in **Table 1**. For dimerization reaction, the calculated negative value of Gibbs free energy change (ΔG) show that the reaction is spontaneous thermodynamically. At room temperature, the equilibrium constant (*K*_{eq}) for dimerization



Scheme 1. Route representing synthesis of pyrrole tosylhydrazones using reactants (1, 2 and 5), product (3: PT and 6: EDTEPC) and byproduct water (4).

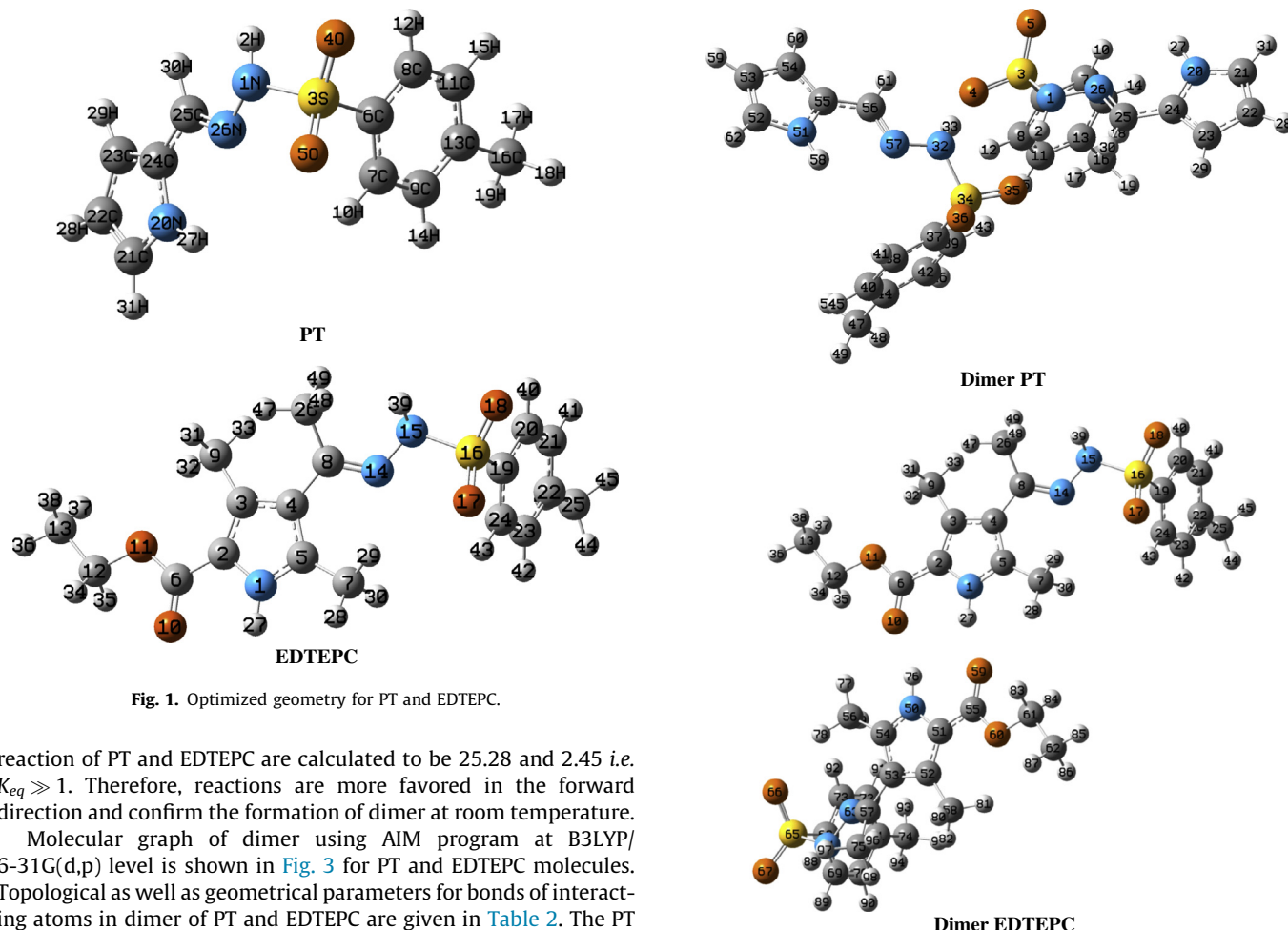


Fig. 1. Optimized geometry for PT and EDTEPC.

reaction of PT and EDTEPC are calculated to be 25.28 and 2.45 i.e. $K_{eq} \gg 1$. Therefore, reactions are more favored in the forward direction and confirm the formation of dimer at room temperature.

Molecular graph of dimer using AIM program at B3LYP/6-31G(d,p) level is shown in Fig. 3 for PT and EDTEPC molecules. Topological as well as geometrical parameters for bonds of interacting atoms in dimer of PT and EDTEPC are given in Table 2. The PT dimer shows two interactions. The interactions N1—H27···O35—S34/N32—H33···O4—S3 in PT is medium classical intermolecular hydrogen bonds due to $(\nabla^2\rho_{BCP}) > 0$ and $H_{BCP} < 0$ in EDTEPC N1—H27···O59—C55/N50—H76···O10—C6 is weak classical intermolecular hydrogen bonds due to $(\nabla^2\rho_{BCP}) > 0$ and $H_{BCP} > 0$. The hydrogen bond energy of N1—H2···O35—S34/N32—H33···O4—S3 in PT found to be -6.554 kcal/mol and in EDTEPC molecule N1—H27···O59—C55/N50—H76···O10—C6 is calculated as -6.2158 kcal/mol. The energy of H—H interaction is calculated as -0.3291, -0.1662 kcal/mol in PT and EDTEPC respectively. The other weaker interactions found in EDTEPC are shown in Table 2.

NMR and UV-Vis spectroscopy

^1H NMR chemical shifts of PT and EDTEPC are calculated using GIAO method and IEFPCM model in $\text{DMSO}-d_6$ as solvent are listed in Table 3 and shown in Supplementary Figure S1(a) and Figure S1(b), respectively. ^1H NMR spectra of PT and EDTEPC show the presence of singlet at 11.503, 11.396 ppm for NH protons of

Fig. 2. Optimized geometry for dimer of PT and EDTEPC.

Table 1

Calculated Enthalpy (H), Gibbs free energy (G) and Entropy (S) of PT and EDTEPC (Monomer, Dimer) and their change for Dimerization, at 25 °C.

Thermodynamic parameters	2xMonomer	Dimer	Dimerization reaction	K_{eq}
<i>PT</i>				
H (a.u.)	−2355.30569	−2355.325298	−0.01961	
G (a.u.)	−2355.436556	−2355.439603	−0.00305	25.28
S (cal/mol K)	275.432	240.575	−34.857	
<i>EDTEPC</i>				
H (a.u.)	−3125.311456	−3125.331257	−0.019801	
G (a.u.)	−3125.492254	−3125.493103	−0.000849	2.4524
S (cal/mol K)	380.526	340.635	−39.891	

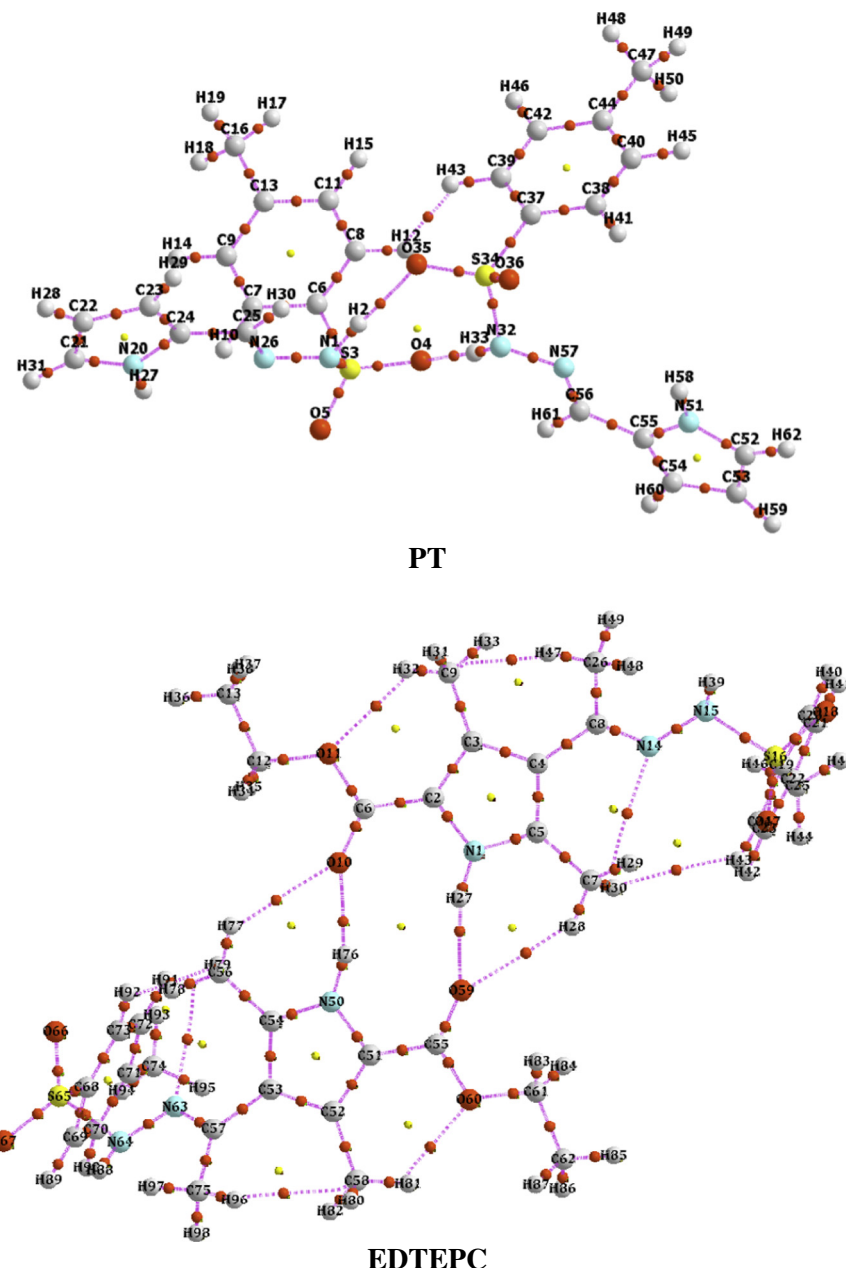


Fig. 3. Molecular graph for dimer of PT and EDTEPC: bond critical points (small red spheres), ring critical points (small yellow sphere), bond paths (pink lines) using AIM program. (For interpretation of the references to color in this figure legend, the reader is referred to the web version of this article.)

pyrrole. The broad singlet at δ 10.172 ppm corresponding to NH proton of hydrazone ($C=NNH$) linkage in EDTEPC. The hydrazone NH proton observed at 9.236 ppm in PT spectrum. A quartet at δ 4.158–4.228 ppm, and a triplet at δ 1.234–1.281 ppm confirm the

presence of methylene and methyl of the ester group in EDTEPC. A singlet at δ 2.101 ppm and 2.065 ppm of methyl groups at 3- and 5-position of pyrrole ring, respectively, in EDTEPC. A singlet at δ 2.003 ppm corresponds to protons of methyl group directly attached

Table 2

Topological parameters for intramolecular interaction: electron density (ρ_{BCP}), Laplacian of electron density ($\nabla^2 \rho_{BCP}$), electron kinetic energy density (G_{BCP}), electron potential energy density (V_{BCP}), total electron energy density (H_{BCP}), Hydrogen bond energy (E_{HB}) at bond critical point (BCP) of PT and EDTEPC.

Interactions	ρ_{BCP}	$\nabla^2 \rho_{BCP}$	G_{BCP}	V_{BCP}	H_{BCP}	E_{HB}
<i>PT</i>						
H12···H43	0.0027	0.0095	-0.0006	-0.0010	-0.0017	-0.3291
H2···O35	0.0277	0.0796	0.0004	-0.0208	-0.0204	-6.5540
O4···H33	0.0277	0.0796	0.0004	-0.0208	-0.0204	-6.5537
<i>EDTEPC</i>						
O10···H76	0.0260	0.0833	0.0203	-0.0198	0.0005	-6.2158
H27···O59	0.0260	0.0832	0.0203	-0.0198	0.0005	-6.2098
H28···O59	0.0067	0.0244	0.0052	-0.0043	0.0009	-1.3460
O10···H77	0.0067	0.0245	0.0052	-0.0043	0.0009	-1.3488
C56···N63	0.0095	0.0356	0.0072	-0.0056	0.0016	-1.7717
C7···N14	0.0095	0.0356	0.0072	-0.0056	0.0016	-1.7720
C9···H47	0.0084	0.0349	0.006	-0.0047	0.0020	-1.4759
C58···H96	0.0084	0.0349	0.0067	-0.0047	0.0020	-1.4777
H30···H43	0.0014	0.0048	0.0008	-0.0005	0.0003	-0.1662
H79···H92	0.0014	0.0047	0.0008	-0.0005	0.0003	-0.1656
O60···H81	0.0126	0.0460	0.0102	-0.0089	0.0012	-2.8112
O11···H32	0.0126	0.046	0.0102	-0.0089	0.0012	-2.8074

ρ_{BCP} , $\nabla^2 \rho_{BCP}$, G_{BCP} , V_{BCP} , H_{BCP} in a.u. and E_{HB} in (kcal/mol)

to carbon of hydrazone (C=NNH) linkage in EDTEPC spectrum. The CH protons of benzene ring are observed at two doublet corresponds to four CH protons of benzene ring. The observed value of two CH protons of benzene ring as a doublet at δ 7.735–7.762 ppm, and other two CH protons at δ 7.376–7.402 ppm which matches well

with the calculated values. In PT, CH=N proton is observed as a singlet at 7.259 ppm. All the calculated chemical shifts corroborate with the observed chemical shifts in EDTEPC and PT except pyrrolic NH. The deshielding in the chemical shift of pyrrole N–H proton designates presence of intermolecular hydrogen-bonding.

To obtain the nature of electronic transitions and absorption, the UV-visible spectra of PT and EDTEPC have been studied by TD/DFT method at same basis set. The calculated electronic transitions of PT and EDTEPC are listed in Table 4 and shown in Fig. 4 and molecular orbital plots in Fig. 5. In EDTEPC, the observed electronic transitions of EDTEPC are observed at $\lambda_{max} = 265$ nm, which correlates well with calculated wavelength at 279 nm. In theoretical UV-Vis spectrum of PT calculated at $\lambda_{max} = 283$ nm, corroborate well with the experimental wavelength at 300 nm. The observed electronic transitions confirm the $\pi \rightarrow \pi^*$ in nature.

Vibrational assignments

The experimental and theoretical (selected) vibrational wavenumbers of PT and EDTEPC, calculated at B3LYP/6-31G(d,p) method and their assignments using PED are given in Tables 5a and 5b. The observed wavenumbers are assigned by comparing the calculated wavenumbers using potential energy distribution (PED) analysis of the various vibrational modes. Comparisons between experimental and theoretical IR spectra for PT and EDTEPC in the region 4000–400 cm⁻¹ are shown in Figs. 6a and 6b, respectively. In majority of the normal modes vibrational wavenumbers are higher than their experimental values. This discrepancies have been corrected

Table 3

Calculated and experimental ¹H NMR chemical shifts (δ /ppm) of PT and EDTEPC in DMSO-d₆ solvent at 25 °C.

PT				EDTEPC			
Atom	$\delta_{calcd.}$	$\delta_{exp.}$	Assignment	Atom	$\delta_{calcd.}$	$\delta_{exp.}$	Assignment
H2	6.6555	9.236	(s, 1H, hydrazone-NH)	H27	9.034	11.396	(s, 1H, pyrrole-NH)
H10	7.8449	6.674–6.620	(t, 4 H, phenyl group)	H28	2.0641	2.065	(s, 1H, methyl-Me3)
H12	7.8504	7.190–7.136		H29	2.7524		
H14	7.4829			H30	2.2788		
H15	7.5326			H31	2.1946	2.101	(s, 1H, methyl-Me2)
H17	2.1853	2.366		H32	2.8439		
H18	2.5696		(s, 3H, —CH ₃)	H33	1.8208		
H19	2.2102			H34	4.2718	4.158–4.228	(q, $J = 7.00$ Hz, 2H, ester-CH ₂)
H27	8.7069	11.503	(s, 1H, pyrrolic NH)	H35	4.2459		
H28	6.2371	6.928–6.902	(d, 3H, pyrrolic CH)	H36	1.1776	1.234–1.281	(t, $J = 7.05$ Hz, 3H, ester methyl-Me1)
H29	6.3312			H37	1.4213		
H30	7.1297	7.259	(s, 1H, —CH=NH, azomethine proton)	H38	1.4483		
H31	6.9571	6.928–6.902	(d, 3H, pyrrolic CH)	H39	7.2276	10.172	(s, 1H, NNH)
				H40	8.1038	7.735–7.762	(d, 2H, Ar—CH)
				H43	7.9637		
				H41	7.774	7.376–7.402	(d, 2H, Ar—CH)
				H42	7.6809		
				H44	2.2247	2.37	(s, 1H, methyl-Me5)
				H45	2.2693		
				H46	2.5644		
				H47	2.1908	2.003	(s, 1H, methyl-Me4)
				H48	1.9569		
				H49	1.6908		

Table 4

Comparison between experimental and calculated electronic excitations: E /eV, oscillatory strength (f), absorption wavelength (λ /nm) at TD-DFT/B3LYP/6-31G(d,p) level of PT and EDTEPC.

S. no.	Excitation	E	f	$(\lambda)_{calcd.}$	$(\lambda)_{exp.}$	Assignment
<i>PT</i>						
1	69 → 72 (H → L + 2)	4.6209	0.1314	268.31		
2	69 → 71 (H → L + 1)	4.3719	0.3146	283.59	234	$\pi \rightarrow \pi^*$
3	69 → 70 (H → L)	3.9102	0.2992	317.08	342	$\pi \rightarrow \pi^*$
<i>EDTEPC</i>						
1	100 → 102 (H → L + 1)	4.4290	0.4971	279.93	265	$\pi \rightarrow \pi^*$
2	99 → 103 (H-1 → L + 3)	5.1650	0.6483	240.05		

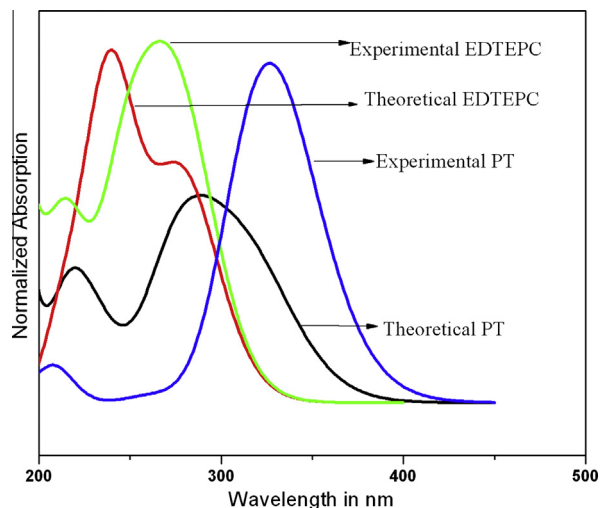


Fig. 4. Comparison between experimental and theoretical UV-Visible spectra for PT and EDTEPC.

by scaling down the calculated wavenumber using scaling factor 0.9608 [33], to discard the anharmonicity present in the real system.

N–H vibrations

In the experimental FT-IR spectrum of PT, the N–H stretch of pyrrole ($\nu_{\text{N–H}}$) is observed at 3490 cm^{-1} , whereas it is calculated at 3528 cm^{-1} . The stretching vibration of hydrazide N–H is observed at 3292 cm^{-1} , whereas this is calculated at 3188 cm^{-1}

in dimer. Therefore, the observed wavenumber at 3292 cm^{-1} is in good agreement with the calculated wavenumber of dimer and indicates the involvement of hydrazide N–H group in hydrogen bonding in the solid phase as observed in our earlier study [26]. The observed hydrazide N–H deformation at 1323 cm^{-1} agrees well with the calculated wavenumber at 1325 cm^{-1} . In the experimental FT-IR spectrum of EDTEPC the N–H stretching vibration of pyrrole ($\nu_{\text{N–H}}$) is observed at 3258 cm^{-1} , correlates well with calculated wavenumber at 3105 cm^{-1} . The observed wavenumber at 3258 cm^{-1} is in good agreement with the hydrogen bonded dimer of pyrrole-2-carboxylic acid recorded in solid state using KBr pellet at 3358 cm^{-1} [34–37]. Therefore, solid state spectrum of EDTEPC attribute to the vibration of hydrogen bonded N–H group. In dimer, the stretching wavenumber of hydrogen bond donor (N–H) is red-shifted due to the elongation of hydrogen bond donor (N–H bond) than the hydrogen bond free N–H group in monomer. The observed N–H wagging mode of pyrrole in EDTEPC compounds at 615 cm^{-1} also indicate the involvement of pyrrole N–H group in intermolecular attraction and correlates with earlier reported wagging mode at 602 cm^{-1} for pyrrole NH in dimer of syn-pyrrole-2-carboxylic acid [34].

C–H vibrations

The pyrrole and benzene rings, in-plane (“ip”) and out-of-plane (“oop”) C–H bending vibrations are reported in literature in the region 3000 – 3100 , 1300 – 1000 and 900 – 675 cm^{-1} , respectively [37]. In the experimental FT-IR spectra of PT and EDTEPC, the observed Ar- ν_{CH} of ring at 3100 , 3027 cm^{-1} corresponds to the calculated wavenumber at 3104 , 3062 cm^{-1} , respectively. The calculated band at 833 , 793 cm^{-1} is attributed to the C–H wagging (an out-of-plane deformation) of benzene ring. In theoretical and observed FT-IR spectra, weak $\nu_{\text{C–H}}$ pyrrole ring are assigned in

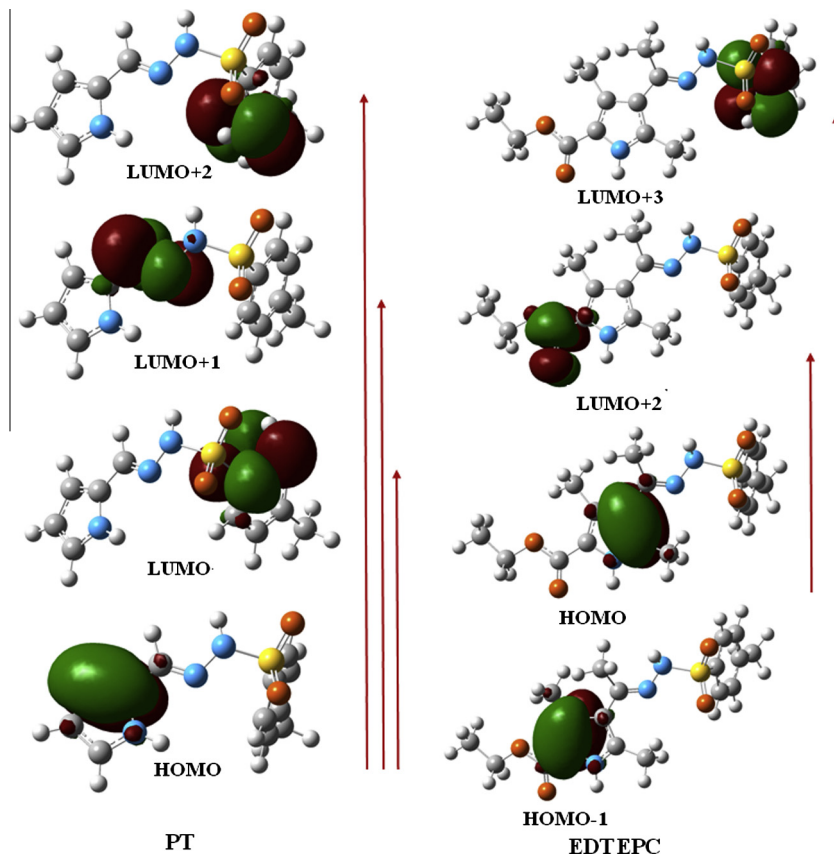


Fig. 5. Molecular orbital plots involved in high oscillator strength electronic excitations for PT and EDTEPC.

Table 5aTheoretical (selected) and experimental vibrational wavenumbers of **PT** and their assignments: wavenumbers (\bar{V}/cm^{-1}), Intensity (km mol $^{-1}$).

Mode no.	\bar{V} Unsc.	\bar{V} Scal.	Intensity	\bar{V} Exp	Assignment (PED) $\geq 5\%$
180	3672	3528	97.63	3490	$\nu(\text{N}20\text{H}27)(86)\nu(\text{N}51\text{H}58)(13)$
178	3318	3188	1353.11	3292	$\nu(\text{N}1\text{H}2)(39)-\nu(\text{N}32\text{H}33)(38)-(\tau\text{-H}2\text{C}56)(5)(\tau\text{-C}25\text{H}33)(5)$
176	3280	3152	2.9		$\nu(\text{C}52\text{H}62)(62)\nu(\text{C}53\text{H}59)(32)$
175	3280	3152	4.08		$\nu(\text{C}21\text{H}31)(62)\nu(\text{C}22\text{H}28)(32)$
174	3264	3136	3.29		$\nu(\text{C}54\text{H}60)(39)-\nu(\text{C}52\text{H}62)(30)\nu(\text{C}53\text{H}59)(28)$
173	3264	3136	4.85		$\nu(\text{C}23\text{H}29)(40)-\nu(\text{C}21\text{H}31)(30)\nu(\text{C}22\text{H}28)(28)$
172	3253	3125	3.63		$\nu(\text{C}54\text{H}60)(54)-\nu(\text{C}53\text{H}59)(37)\nu(\text{C}52\text{H}62)(6)$
171	3253	3125	5.55		$\nu(\text{C}23\text{H}29)(54)-\nu(\text{C}22\text{H}28)(38)\nu(\text{C}21\text{H}31)(6)$
170	3231	3104	1.11		$\nu(\text{C}38\text{H}41)(29)-\nu(\text{C}39\text{C}42)(25)-(\delta\text{-as-R}4)(21)\nu(\text{C}37\text{C}38)(12)$
169	3231	3104	2.82	3100	$\nu(\text{C}7\text{H}10)(79)\nu(\text{C}38\text{H}41)(6)-\nu(\text{C}39\text{C}42)(5)$
168	3224	3098	2.98		$\nu(\text{C}8\text{H}12)(37)4\nu(\text{S}3\text{C}6)(25)-(\delta\text{-as-R}4)(19)-(\delta\text{-as-R}4)(10)$
167	3224	3098	0.26		$4\nu(\text{S}3\text{C}6)(32)-(\delta\text{-as-R}4)(24)-\nu(\text{C}8\text{H}12)(22)-(\delta\text{-as-R}4)(13)(\tau\text{-C}40\text{C}43)(5)$
166	3186	3061	11.24		$\nu(\text{C}9\text{H}14)(85)\nu(\text{C}11\text{H}15)(5)$
165	3186	3061	14.22		$\nu(\text{C}40\text{C}45)(25)-\nu(\text{C}40\text{C}44)(19)-(\delta\text{-as-R}4)(15)-\nu(\text{C}38\text{H}41)(14)-\delta(\text{C}37\text{C}39\text{H}43)(13)-(\delta\text{-as-R}4)(9)$
164	3185	3060	16.7		$\delta(\text{C}37\text{C}39\text{H}43)(61)-(\delta\text{-as-R}4)(11)-\nu(\text{C}42\text{H}46)(9)-\nu(\text{C}11\text{H}15)(6)\nu(\text{C}42\text{C}44)(5)$
163	3184	3059	9.54		$\delta(\text{C}37\text{C}39\text{H}43)(57)+\delta(\text{C}11\text{H}15)(14)-(\delta\text{-as-R}4)(10)-\nu(\text{C}42\text{H}46)(9)$
162	3132	3009	10.81		$\nu(\text{C}16\text{H}17)(57)-\nu(\text{C}16\text{H}18)(41)$
161	3132	3009	13.43		$\nu(\text{C}47\text{H}48)(58)-\nu(\text{C}47\text{H}49)(38)$
160	3105	2984	10.66	2994	$\nu(\text{C}56\text{H}61)(95)$
159	3105	2984	17.31	2975	$\nu(\text{C}25\text{H}30)(95)$
158	3104	2982	17.54		$\nu(\text{C}16\text{H}19)(40)-\nu(\text{C}16\text{H}18)(37)-\nu(\text{C}16\text{H}17)(22)$
157	3104	2982	16.7		$\nu(\text{C}47\text{C}50)(41)-\nu(\text{C}47\text{H}49)(39)-\nu(\text{C}47\text{H}48)(20)$
156	3042	2923	25.31	2925	$\nu(\text{C}47\text{C}50)(58)\nu(\text{C}47\text{H}49)(21)\nu(\text{C}47\text{H}48)(19)$
155	3042	2923	19.18	2926	$\nu(\text{C}16\text{H}19)(58)\nu(\text{C}16\text{H}18)(20)\nu(\text{C}16\text{H}17)(19)$
154	1685	1619	115.07	1677	$(\rho\text{-C}56\text{N}57\text{H}61)(33)-\nu(\text{C}56\text{N}57)(13)(\tau\text{-O}4\text{C}56)(9)-(\rho\text{-C}25\text{N}26\text{H}30)(7)-(\tau\text{-C}40\text{C}43)(6)\nu(\text{C}25\text{N}26)(6)-\delta(\text{C}37\text{C}39\text{H}43)(6)$
153	1685	1619	25.49	1618	$(\rho\text{-C}56\text{N}57\text{H}61)(30)-\nu(\text{C}56\text{N}57)(12)(\rho\text{-C}25\text{N}26\text{H}30)(11)-\nu(\text{C}25\text{N}26)(9)(\tau\text{-O}4\text{C}56)(8)-(\tau\text{-C}25\text{H}33)(5)-(\tau\text{-H}2\text{C}56)(5)$
152	1654	1590	25.39		$(\tau\text{-C}40\text{C}43)(54)\delta(\text{C}37\text{C}39\text{H}43)(38)$
151	1654	1589	12.98	1588	$\nu(\text{C}=\text{N})(54)\delta(\text{C}37\text{C}39\text{H}43)(38)$
150	1627	1563	1.18	1564	$(\tau\text{-C}40\text{C}43)(51)\delta(\text{C}37\text{C}39\text{H}43)(41)$
149	1627	1563	3.8	1578	$(\tau\text{-C}40\text{C}43)(51)\delta(\text{C}37\text{C}39\text{H}43)(41)$
148	1607	1544	0.33		$\delta(\text{N}1\text{H}2\text{S}3)(36)-(\tau\text{-H}2\text{C}56)(14)-(\tau\text{-C}25\text{H}33)(14)\delta(\text{N}32\text{H}33\text{S}34)(12)$
147	1606	1543	5.67	1514	$\delta(\text{N}1\text{H}2\text{S}3)(36)-\delta(\text{N}32\text{H}33\text{S}34)(12)-(\tau\text{-H}2\text{C}56)(11)(\tau\text{-C}25\text{H}33)(10)$
146	1536	1475	9.93		$\delta(\text{C}37\text{C}39\text{H}43)(57)(\tau\text{-C}40\text{C}43)(42)$
145	1535	1475	4.06		$\delta(\text{C}37\text{C}39\text{H}43)(57)(\tau\text{-C}40\text{C}43)(42)$
144	1531	1471	19.8		$\delta(\text{N}1\text{H}2\text{S}3)(32)-\delta(\text{C}37\text{C}39\text{H}43)(19)-(\tau\text{-C}40\text{C}43)(14)\delta(\text{N}32\text{H}33\text{S}34)(10)-(\tau\text{-H}2\text{C}56)(9)-(\tau\text{-C}25\text{H}33)(9)$
143	1514	1454	194.38		$\delta(\text{N}1\text{H}2\text{S}3)(41)-(\tau\text{-H}2\text{C}56)(16)(\tau\text{-C}25\text{H}33)(16)-\delta(\text{N}32\text{H}33\text{S}34)(13)\delta(\text{N}1\text{N}26)(5)$
142	1505	1446	7.2	1451	$\delta(\text{C}37\text{C}39\text{H}43)(52)-\nu(\text{C}37\text{C}38)(22)-\nu(\text{C}38\text{H}41)(9)-(\delta\text{-as-R}4)(5)$
141	1505	1446	7.2		$(\delta\text{-as-Me})(46)(\delta\text{-as-Me})(14)-\delta(\text{N}1\text{H}2\text{S}3)(12)-(\rho\text{-Me})(6)$
140	1502	1443	6.24	1444	$(\delta\text{-as-Me})(68)-(\delta\text{-as-Me})(17)-(\rho\text{-Me})(7)$
139	1501	1442	6.97		$\delta(\text{C}37\text{C}39\text{H}43)(19)-\nu(\text{C}38\text{H}41)(18)-(\delta\text{-as-Me})(14)-(\text{R4-Puckering})(14)(\tau\text{-R}4)(12)-\nu(\text{C}37\text{C}38)(9)$
138	1492	1434	1.33		$\delta(\text{N}1\text{H}2\text{S}3)(45)\nu(\text{N}32\text{H}33\text{S}34)(15)-(\tau\text{-H}2\text{C}56)(13)-(\tau\text{-C}25\text{H}33)(13)\delta(\text{N}1\text{N}26)(7)$
137	1486	1428	21.3		$\delta(\text{N}1\text{H}2\text{S}3)(42)-(\tau\text{-H}2\text{C}56)(15)(\tau\text{-C}25\text{H}33)(15)-\delta(\text{N}32\text{H}33\text{S}34)(14)\delta(\text{N}1\text{N}26)(5)$
136	1469	1412	8.53		$\delta(\text{N}1\text{H}2\text{S}3)(32)\delta(\text{N}32\text{H}33\text{S}34)(11)-(\tau\text{-C}25\text{H}33)(8)-(\tau\text{-H}2\text{C}56)(8)-\nu(\text{N}51\text{C}55)(5)$
135	1469	1412	48.77		$\delta(\text{N}1\text{H}2\text{S}3)(25)-(\tau\text{-H}2\text{C}56)(11)(\tau\text{-C}25\text{H}33)(10)-\delta(\text{N}32\text{H}33\text{S}34)(8)-\nu(\text{N}20\text{C}24)(5)$
134	1466	1409	2.92		$\delta(\text{N}1\text{H}2\text{S}3)(43)-(\tau\text{-H}2\text{C}56)(15)-(\tau\text{-C}25\text{H}33)(15)\delta(\text{N}32\text{H}33\text{S}34)(14)\delta(\text{N}1\text{N}26)(5)$
133	1463	1405	5.8		$\delta(\text{N}1\text{H}2\text{S}3)(41)-(\tau\text{-H}2\text{C}56)(14)(\tau\text{-C}25\text{H}33)(14)-\delta(\text{N}32\text{H}33\text{S}34)(13)\delta(\text{C}37\text{C}39\text{H}43)(5)\delta(\text{N}1\text{N}26)(5)$
132	1441	1385	3.22	1382	$\delta(\text{C}37\text{C}39\text{H}43)(56)(\tau\text{-C}40\text{C}43)(42)$
131	1441	1384	13.94	1379	$\delta(\text{C}37\text{C}39\text{H}43)(56)(\tau\text{-C}40\text{C}43)(42)$
130	1427	1371	0.21		$(\tau\text{-C}40\text{C}43)(44)\delta(\text{C}37\text{C}39\text{H}43)(26)-(\delta\text{-as-Me})(17)$
129	1427	1371	0.75		$(\delta\text{-as-Me})(55)(\tau\text{-C}40\text{C}43)(19)\delta(\text{C}37\text{C}39\text{H}43)(8)-(\delta\text{-as-Me})(6)\nu(\text{C}13\text{C}16)(5)$
128	1379	1325	6.98	1323	$(\tau\text{-C}40\text{C}43)(23)\delta(\text{C}37\text{C}39\text{H}43)(17)-\delta(\text{N}1\text{H}2\text{S}3)(17)-(\tau\text{-H}2\text{C}56)(11)-(\tau\text{-C}25\text{H}33)(11)\delta(\text{N}32\text{H}33\text{S}34)(6)$
127	1373	1319	43.25	1319	$\delta(\text{N}1\text{H}2\text{S}3)(31)-(\tau\text{-C}40\text{C}43)(16)-\delta(\text{C}37\text{C}39\text{H}43)(16)-\delta(\text{N}32\text{H}33\text{S}34)(10)-(\tau\text{-H}2\text{C}56)(6)(\tau\text{-C}25\text{H}33)(6)$
126	1352	1299	0.17		$(\tau\text{-C}40\text{C}43)(47)\delta(\text{C}37\text{C}39\text{H}43)(39)\nu(\text{C}40\text{C}44)(5)$
125	1352	1299	3.26		$(\tau\text{-C}40\text{C}43)(47)\delta(\text{C}37\text{C}39\text{H}43)(38)\nu(\text{C}40\text{C}44)(5)$
124	1335	1283	0.14		$\delta(\text{C}37\text{C}39\text{H}43)(51)(\tau\text{-C}40\text{C}43)(49)$
123	1335	1282	2.99	1279	$\nu(\text{S=O})(51)(\tau\text{-C}40\text{C}43)(49)$
122	1323	1271	66.2		$(\tau\text{-C}40\text{C}43)(50)\delta(\text{C}37\text{C}39\text{H}43)(45)$
121	1323	1271	8.85	1274	$(\rho\text{-C}56\text{N}57\text{H}61)(39)(\rho\text{-C}25\text{N}26\text{H}30)(10)(\tau\text{-O}4\text{C}56)(8)\delta(\text{C}37\text{C}39\text{H}43)(5)(\tau\text{-C}40\text{C}43)(5)$
120	1316	1264	337.45		$(\tau\text{-C}40\text{C}43)(49)\delta(\text{C}37\text{C}39\text{H}43)(40)$
119	1316	1264	55.36		$(\tau\text{-C}40\text{C}43)(50)\delta(\text{C}37\text{C}39\text{H}43)(45)$
118	1277	1227	4.17	1233	$\nu_{\text{as}}(\text{S=O})(55)+\delta(\text{N}1\text{H}2\text{S}3)(31)$
117	1277	1227	14.44		$(\rho\text{-C}56\text{N}57\text{H}61)(30)\delta(\text{N}32\text{H}33\text{S}34)(14)-(\tau\text{-C}25\text{H}33)(13)(\tau\text{-O}4\text{C}56)(6)-\delta(\text{C}53\text{C}54\text{H}60)(5)-\delta(\text{N}1\text{H}2\text{S}3)(5)$
116	1235	1187	0.85	1189	$\delta(\text{C}37\text{C}39\text{H}43)(48)(\tau\text{-C}40\text{C}43)(46)$
115	1235	1187	2.37	1188	$(\tau\text{-C}40\text{C}43)(47)\delta(\text{C}37\text{C}39\text{H}43)(46)$
114	1213	1165	2.98		$\delta(\text{C}37\text{C}39\text{H}43)(54)(\tau\text{-C}40\text{C}43)(45)$
113	1210	1162	0.89		$\delta(\text{C}37\text{C}39\text{H}43)(54)(\tau\text{-C}40\text{C}43)(45)$
112	1147	1102	18.07		$(\tau\text{-C}40\text{C}43)(56)\delta(\text{C}37\text{C}39\text{H}43)(43)$
111	1147	1102	4.94	1108	$\nu(\text{S=O})(55)\delta(\text{C}37\text{C}39\text{H}43)(44)$
110	1144	1099	3.87		$(\tau\text{-C}40\text{C}43)(55)\delta(\text{C}37\text{C}39\text{H}43)(44)$
109	1142	1097	12.99		$(\tau\text{-C}40\text{C}43)(55)\delta(\text{C}37\text{C}39\text{H}43)(45)$
108	1135	1091	392.34		$(\tau\text{-C}40\text{C}43)(64)\delta(\text{C}37\text{C}39\text{H}43)(27)$
107	1130	1086	125.55		$(\tau\text{-C}40\text{C}43)(63)\delta(\text{C}37\text{C}39\text{H}43)(31)$
106	1120	1076	18.65		$(\tau\text{-C}40\text{C}43)(60)\delta(\text{C}37\text{C}39\text{H}43)(33)$

(continued on next page)

Table 5a (continued)

Mode no.	V Unsc.	V Scal.	Intensity	V Exp	Assignment (PED) $\geq 5\%$
105	1120	1076	166.5		(τ -C40C43)(59) δ (C37C39H43)(37)
104	1103	1059	78.77		(τ -C40C43)(51) δ (C37C39H43)(32)
103	1102	1059	4.43		(τ -C40C43)(57) δ (C37C39H43)(33)
102	1085	1042	323.13		(τ -C40C43)(63) δ (C37C39H43)(35)
101	1071	1029	4.71		(τ -C40C43)(62) δ (C37C39H43)(36)
100	1065	1024	14.18		(R4-Puckering)(44)-(τ -R4)(29)(τ -C40C43)(16) δ (C37C39H43)(5)(ω -C39H43)(5)
99	1065	1024	14.52		(τ -C40C43)(39) δ (C37C39H43)(27)-(p-Me)(16)
98	1063	1022	127.65		(τ -C40C43)(59) δ (C37C39H43)(26)
97	1063	1021	16.94	1021	(τ -C40C43)(60) δ (C37C39H43)(34)
96	1033	992	0.44	998	(τ -C40C43)(60) δ (C37C39H43)(35)
95	1033	992	23.33	992	(τ -C40C43)(68) δ (C37C39H43)(28)
94	1014	974	0.55		(τ -C40C43)(61) δ (C37C39H43)(18)(ω -C39H43)(11)
93	1014	974	0.62		(τ -C40C43)(60) δ (C37C39H43)(32)
92	999.3	960	0.61		(τ -H2C56)(33)-(τ -C25H33)(33)- δ (N1H2S3)(8)
91	999.1	960	2.45		δ (N1H2S3)(17)-(τ -H2C56)(12)-(τ -C25H33)(11)- δ (N1N26)(11) δ (N32HH33S34)(5)-(ω -C39H43)(5)+ ω (C25H30)(5)
90	985.6	947	0.21	943	(ω -C39H43)(63)(τ -C40C43)(36)
89	977.9	940	1.73		(ω -C39H43)(64)(τ -C40C43)(32)
88	973	935	0.28		(ω -C39H43)(49)(τ -C40C43)(42)
87	970.5	932	2.96		(ω -C39H43)(58)(τ -C40C43)(37)
86	970.2	932	22.3		ω (C25H30)(33)(τ -H2C56)(22) ω (C56H61)(20)(τ -C25H33)(19)
85	970	932	2.8		ω (C39H43)(27)+ ω (C25H30)(21)(τ -C40C43)(19)(τ -C25H33)(11)-(τ -H2C56)(10)- ω (C56H61)(9)
84	917	881	88.83	896	(τ -H2C56)(30)(τ -C25H33)(29)+ δ (N1N26)(15)- δ (N1H2S3)(7) δ (N57N32)(5)
83	914.2	878	309.77		(τ -H2C56)(26)-(τ -C25H33)(25) δ (N1N26)(15)- δ (N1H2S3)(9)- δ (N57N32)(5)
82	896.9	862	0.18		(τ -H2C56)(22)-(τ -C25H33)(20) δ (N1N26)(17)- δ (R1)(7) δ (R3)(6)
81	896.9	862	7.1		(τ -C25H33)(22)-(τ -H2C56)(21)- δ (N1N26)(13)+ δ (R3)(7)- δ (R1)(6)
77	852.7	819	3.36	833	(ω -C39H43)(53)(τ -C40C43)(47)
76	829.9	797	1.65		(ω -C39H43)(68)(τ -C40C43)(27)
75	828.1	796	23.66	792	(ω -C39H43)(70)(τ -C40C43)(26)
74	815.9	784	10.03	778	(τ -C40C43)(75) δ (C37C39H43)(10)-(δ as-R4)(7)(ω -C39H43)(6)
73	815.2	783	11.45		(τ -C40C43)(72)(ω -C39H43)(16) δ (C37C39H43)(6)-(δ as-R4)(4)
72	809.1	777	44.41		ω (C25H30)(25)(τ -C25H33)(23)-(τ -C40C43)(16)(τ -H2C56)(11) ω (C56H61)(7)-(ω -C39H43)(5)
71	809	777	2.63	773	(τ -C40C43)(35)-(τ -H2C56)(16)(ω -C39H43)(15)(τ -C25H33)(10) ω (C25H30)(7)- ω (C56H61)(7)
70	788.4	758	4.53	749	δ (N1N26)(31)(τ -H2C56)(25)(τ -C25H33)(22) δ (N57N32)(10)
69	782.9	752	35.89	757	(τ -C25H33)(25)- δ (N1N26)(24)-(τ -H2C56)(23) δ (N57N32)(9)
68	734.2	705	170.38		δ (N1N26)(29)(τ -H2C56)(24)(τ -C25H33)(23) δ (N57N32)(10)
67	733.9	705	6.69		ω (C52H62)(13)- ω (C21H31)(13) ω (C25H30)(12)-(R4-Puckering)(12) δ (N1N26)(9)(τ -C40C43)(7)- ω (C56H61)(6)
66	724.8	696	206.93	694	(R4-Puckering)(29)- δ (N1N26)(24)-(τ -H2C56)(14)-(τ -C25H33)(13)- δ (N57N32)(8)-(τ -C40C43)(5)
65	714.1	686	14.05		(R4-Puckering)(64)(ω -C39H43)(30)
64	710.9	683	50.36		(R4-Puckering)(50)(ω -C39H43)(40)
63	683.9	657	8.9	656	(τ -C25N26)(41)-(τ -C56N57)(19) δ (N1N26)(14)- ω (C25H30)(10)- δ (N57N32)(5) ω (C56H61)(5)
62	683.1	656	2.09		(τ -C25N26)(36)(τ -C56N57)(20)-(ω -C39H43)(12)- ω (C25H30)(9)-(R4-Puckering)(6)- ω (C56H61)(5)
61	659.9	634	132.63		δ (N1N26)(29)(τ -H2C56)(19)-(τ -C25H33)(19)- δ (N57N32)(10)-(τ -C40C43)(7)-(ω -C39H43)(5)
60	648.9	623	0.02	624	(τ -C40C43)(69)(δ as-R4)(22) δ (C37C39H43)(6)
59	648.1	623	1.34		(τ -C40C43)(64)(δ as-R4)(26) δ (C37C39H43)(7)
58	644	619	38.15		(δ as-R4)(27)(τ -H2C56)(20)(τ -C25H33)(19) δ (N1N26)(15) δ (N57N32)(5)
57	631.9	607	22.61		δ (N1N26)(30)(τ -H2C56)(23)-(τ -C25H33)(23)- δ (N57N32)(10)
56	631.1	606	1.93		(τ -C25N26)(30)(τ -C56N57)(18)(τ -C25H33)(10)- δ (R3)(10)- δ (R1)(9)
55	629.8	605	46.46		δ (N1N26)(27)(τ -H2C56)(26)-(τ -C25H33)(26)- δ (N57N32)(9)
54	586.1	563	188.21	558	δ (N1N26)(19)(τ -C40C43)(17)(ω -C39H43)(15)(τ -H2C56)(14)-(τ -C25H33)(14)- δ (R4)(9)- δ (N57N32)(6)
53	576.3	554	18.58		(τ -C40C43)(35)(ω -C39H43)(21)-(τ -R4)(16)- δ (N1N26)(10)
52	550	528	143.19		(τ -C40C43)(33)-(δ as-R4)(25)(τ -C25N26)(11) δ (C37C39H43)(9)- ω (C25H30)(7)
51	549.6	528	16.78		(τ -C40C43)(29)-(τ -R4)(18)(τ -C56N57)(10)-(t-C25N26)(9)- ω (C56H61)(7)(ω -C39H43)(6) ω (C25H30)(6)
50	548.7	527	38.8		(δ as-R4)(37)-(τ -R4)(24)- δ (C37C39H43)(12)(ω -C39H43)(8)-(τ -C40C43)(8)
49	548.1	527	49.99		(δ as-R4)(36)-(τ -C40C43)(22)-(τ -R4)(12)- δ (C37C39H43)(10)- δ (N1N26)(8)
48	522.7	502	4.54		(τ -C40C43)(68)-(τ -R4)(24)
47	519.5	499	41.3	482	(τ -C40C43)(67)-(τ -R4)(23)(ω -C39H43)(5)
46	477.8	459	9.02		(τ -R4)(51)-(τ -C40C43)(44)
45	477.5	459	1.82	456	(τ -R4)(52)-(τ -C40C43)(43)
44	436.2	419	1.44	427	(τ -R4)(35)-(τ -R4)(10)(δ as-R4)(8) δ (C37C39H43)(6)(R4-Puckering)(5)

Proposed assignment and potential energy distribution (PED) for vibrational modes: types of vibrations: v – stretching, δ sc – scissoring, ρ – rocking, ω – wagging, t – twisting, δ – deformation, δ s – symmetric deformation, δ as – asymmetric deformation, δ ip – in plane deformation, δ oop – out of plane deformation, τ – torsion, R₁ and R₃ – pyrrole ring, R₂ and R₄ – phenyl ring, Me – methyl on phenyl ring.

the range of 3128–3143 cm⁻¹ in both PT and EDTEPC. The CH₃ group associate with six types of vibrational frequencies namely: symmetric stretch (v_s), asymmetric stretch (v_{as}), scissoring (δ sc), rocking (ρ), wagging (ω) and twisting (t), according to internal coordinate system recommended by Pulay et al. [38]. As we know that scissoring and rocking deformations belong to polarized in-plane vibration, whereas wagging and twisting deformations belong to depolarized out-of-plane vibration. In EDTEPC five methyl groups are present. Out of five two of them are directly

attached to the pyrrole ring, remaining is attached to the CH₂ of ester group, azomethine carbon and benzene ring. The C–H stretching vibrations of methyl groups and CH₂ of ester group are observed at 2925 cm⁻¹ and is also corresponds with the earlier reported absorption band at 2990–2850 cm⁻¹ in the region [39]. The observed wavenumbers in the region 1423 cm⁻¹ designates in-plane deformation mode of methyl groups. The observed wavenumbers at 774 cm⁻¹ assign to the out-of-plane deformation mode of methyl groups. The observed wavenumber at 774 cm⁻¹,

Table 5bTheoretical (selected) and experimental vibrational wavenumbers of EDTEPC and their assignments: wavenumbers (\bar{V}/cm^{-1}), intensity (km mol $^{-1}$).

Mode no.	\bar{V} Unsc.	\bar{V} Scal.	Intensity	\bar{V} Exp.	Assignment (PED) $\geq 5\%$
141	3649	3505	108.62	3386	$\nu(\text{N1H27})(9) + \text{C24H43}(20)$
140	3437	3303	10.93		$\nu(\text{N15H39})(90) - (\rho-\text{N15N14S16})(8)$
139	3231	3105	1.11	3258	$\nu(\text{C24H43})(97)$
138	3224	3097	1.46		$\nu(\text{C20H40})(96)$
137	3187	3062	10.38	3027	$\nu(\text{C23H42})(91) - \nu(\text{C21H41})(5)$
136	3186	3061	14.59		$\nu(\text{C21H41})(90) - \nu(\text{C23H42})(6)$
135	3184	3059	7.95		$\nu(\text{C26H47})(93) - \nu(\text{C26H49})(5)$
134	3161	3037	6.68		$\nu(\text{C9H32})(84) - \nu(\text{C9H33})(13)$
133	3161	3037	1.93		$\nu(\text{C7H29})(87) - \nu(\text{C7H28})(10)$
132	3138	3015	35.49		$\nu(\text{C13H38})(46) - \nu(\text{C13H37})(38) - \nu(\text{C12H35})(8) \nu(\text{C12H34})(7)$
131	3132	3009	12.43		$\nu(\text{C25H44})(51) - \nu(\text{C25H45})(48)$
130	3130	3008	28.44	2992	$\nu(\text{C13H36})(64) - \nu(\text{C13H37})(20) - \nu(\text{C13H38})(14)$
129	3105	2984	7.83		$\nu(\text{C12H34})(43) - \nu(\text{C12H35})(41) \nu(\text{C13H37})(8) - \nu(\text{C13H38})(8)$
128	3104	2982	18		$\nu(\text{C25H46})(40) - \nu(\text{C25H45})(31) - \nu(\text{C25H44})(29)$
127	3102	2980	18.35	2925	$\nu(\text{C9H33})(70) - \nu(\text{C9H31})(21) \nu(\text{C9H32})(8)$
126	3096	2974	24.12	2816	$\nu(\text{C7H28})(51) - \nu(\text{C7H30})(47)$
125	3082	2961	9.59		$\nu(\text{C26H49})(73) - \nu(\text{C26H48})(24)$
124	3066	2946	23.17		$\nu(\text{C12H35})(50) \nu(\text{C12H34})(48)$
123	3056	2936	16.84		$\nu(\text{C13H36})(35) \nu(\text{C13H37})(33) \nu(\text{C13H38})(32)$
122	3042	2923	22.17	2707	$\nu(\text{C25H46})(57) \nu(\text{C25H45})(18) \nu(\text{C25H44})(18)$
121	3042	2923	24.74		$\nu(\text{C7H30})(48) \nu(\text{C7H28})(37) \nu(\text{C7H29})(8)$
120	3037	2918	29.19		$\nu(\text{C9H31})(78) \nu(\text{C9H33})(16) \nu(\text{C9H32})(6)$
119	3023	2904	11.94		$\nu(\text{C26H48})(75) \nu(\text{C26H49})(20)$
118	1759	1690	409.12	1665	$\nu(\text{C6O10})(85)$
117	1665	1600	12.64	1598	$\nu(\text{C8N14})(67) (\delta-\text{C8N14N15})(8)$
116	1655	1590	21.59		$\nu(\text{C20C21})(21) \nu(\text{C23C24})(21) (\delta\text{as-R1})(10) - \nu(\text{C22C23})(8) - \nu(\text{C21C22})(7) \delta(\text{C22H42C23})(7)$
115	1629	1565	1.18		$\nu(\text{C19C24})(20) - (\delta\text{as-Me1})(19) \nu(\text{C21C22})(17) - \nu(\text{C22C23})(17) (\delta\text{as-R1})(9)$
114	1606	1543	88.16	1566	$\nu(\text{C2C3})(28) - \nu(\text{C4C5})(18) - \delta(\text{C2H27N1})(10) - \nu(\text{C2C6})(7) \nu(\text{C4C8})(5) - \nu(\text{C8N14})(5)$
113	1550	1489	68.27	1515	$\nu(\text{C2C3})(18) \nu(\text{N1C5})(17) - \nu(\text{C5C7})(12) \nu(\text{C4C5})(7) \delta(\text{C2H27N1})(7) - \nu(\text{N1C2})(6) \delta(\text{R})(5)$
112	1536	1476	4.52		$\delta(\text{C19H40C20})(15) (\omega-\text{C24H43})(14) - \delta(\text{C22H42C23})(11) \delta(\text{C20H41C21})(11) - (\delta\text{as-Me1})(9) \nu(\text{C19C24})(9) \nu(\text{C21C22})(7) \nu(\text{C22C23})(6)$
111	1536	1476	12.77	1492	$\nu(\text{N1C5})(13) - (\delta\text{as-Me2})(10) \nu(\text{C4C8})(9) - \nu(\text{C3C4})(8) - \nu(\text{C4C5})(6) - (\delta\text{as-Me3})(6)$
110	1533	1472	8.99		$(\delta\text{sc-CH2})(59) \nu(\text{N1H27})(15) (\delta\text{as-Me1})(5) \nu(\text{C2C3})(4)$
109	1517	1457	9.09		$(\delta\text{as-Me4})(43) - (\delta\text{as-Me2})(15) (\delta\text{as-Me3})(15) - (\delta\text{as-Me3})(7)$
108	1513	1454	0.72		$5\nu(\text{N1H27})(37) - (\delta\text{sc-CH2})(18) - (\delta\text{as-Me3})(13) (\delta\text{as-Me1})(10) - (\delta\text{as-Me3})(7) (\delta\text{as-Me4})(6)$
107	1510	1450	8.29		$(\delta\text{as-Me3})(36) (\delta\text{as-Me3})(15) - (\delta\text{sc-CH2})(11) \nu(\text{N1H27})(11) - (\delta\text{as-Me4})(6) (\delta\text{as-Me1})(6)$
106	1504	1445	13.36		$(\delta\text{as-Me5})(81) - (\rho-\text{Me5})(6)$
105	1503	1444	10.36		$(\delta\text{as-Me4})(41) - \delta(\text{as-Me3})(12) (\delta\text{as-Me3})(9) - (\delta\text{as-Me2})(5)$
104	1503	1444	5.71		$(\delta\text{as-Me5})(89) - (\rho-\text{Me5})(6)$
103	1501	1442	4.99		$(\delta\text{as-Me1})(63) - \nu(\text{N1H27})(21) - (\rho-\text{Me1})(7)$
102	1493	1434	20.46	1423	$(\delta\text{as-Me3})(33) (\delta\text{as-Me4})(22) (\delta\text{as-Me2})(16) (\delta\text{as-Me2})(5) - (\delta\text{as-Me4})(5)$
101	1489	1431	6.34		$(\delta\text{as-Me2})(50) (\delta\text{as-Me4})(12) - (\delta\text{as-Me3})(5) - \nu(\text{N1C2})(5)$
100	1480	1422	55.19		$(\delta\text{as-Me2})(29) (\delta\text{as-Me4})(16) - (\delta\text{as-Me2})(15) \nu(\text{C4C8})(8) - (\delta\text{as-Me3})(5) - \nu(\text{C3C4})(5)$
99	1469	1411	224.46	1420	$\nu(\text{N1C2})(14) - \nu(\text{C2C6})(13) (\delta\text{as-Me2})(10) \delta(\text{R})(25)$
98	1442	1385	9.36		$\nu(\text{C23C24})(21) - \nu(\text{C20C21})(20) \delta(\text{C20H41C21})(11) \delta(\text{C22H42C23})(11) (\delta\text{as-Me5})(9) (\omega-\text{C24H43})(8) - \delta(\text{C19H40C20})(8) \delta(\text{C21C25C22})(5)$
97	1437	1381	13.72		$(\delta\text{S-Me1})(45) - (\delta\text{S-Me2})(16) - (\omega-\text{CH2})(14) \nu(\text{C12C13})(10)$
96	1432	1376	1.5		$(\delta\text{S-Me3})(76) \nu(\text{C3C9})(7) (\delta\text{S-Me2})(6)$
95	1427	1371	47.25		$(\delta\text{S-Me2})(56) (\delta\text{S-Me1})(21) - (\delta\text{S-Me3})(5)$
94	1427	1371	1.09		$(\delta\text{S-Me5})(88) \nu(\text{C22C25})(8)$
93	1417	1361	29.68		$8\nu(\text{C4C8})(63) - (\rho-\text{N15N14S16})(15)$
92	1401	1346	14.81		$(\omega-\text{CH2})(23) - (\rho-\text{N15N14S16})(14) (\delta\text{S-Me1})(11) \nu(\text{C3C4})(9) - \nu(\text{C4C5})(8) - \delta(\text{R})(5)$
91	1394	1340	1.44		$(\rho-\text{N15N14S16})(38) (\omega-\text{CH2})(20) \nu(\text{C4C8})(11) (\delta\text{S-Me1})(6) - \nu(\text{N1C5})(3)$
90	1380	1326	22.71	1305	$(\rho-\text{N15N14S16})(25) \nu(\text{C3C4})(14) \nu(\text{N1C5})(10) - \nu(\text{C4C5})(6) - (\omega-\text{CH2})(6) - \delta(\text{R})(5) - \nu(\text{C4C8})(5)$
89	1354	1301	2.19		$\nu(\text{C22C23})(18) - \nu(\text{C21C22})(18) \nu(\text{C19C24})(15) - (\delta\text{as-Me1})(15) \nu(\text{C20C21})(10) - \nu(\text{C23C24})(9)$
88	1335	1283	3.57		$\delta(\text{C19H40C20})(21) - (\omega-\text{C24H43})(20) \delta(\text{C22H42C23})(19) \delta(\text{C20H41C21})(18) (\delta\text{as-Me1})(5) - \nu(\text{C19C24})(5)$
87	1322	1270	104.61	1285	$\nu(\text{S16O17})(36) - \nu(\text{S16O18})(31) - (\rho-\text{N15N14S16})(5)$
86	1298	1248	48.97		$(\text{t-CH2})(18) - \nu(\text{N1C2})(18) \nu(\text{C4C8})(9) \nu(\text{C3C4})(7) \nu(\text{C8C26})(7) \nu(\text{C3C9})(5) \delta(\text{N14C4C8})(5)$
85	1298	1247	15.73		$(\text{t-CH2})(61) (\rho-\text{Me1})(8) \nu(\text{N1C2})(4) \nu(\text{C4C8})(3) \nu(\text{C3C4})(3) - \nu(\text{C8C26})(2)$
84	1284	1234	762.06	1233	$\nu(\text{C6O11})(25) \delta(\text{C22H27N1})(13) - \nu(\text{C2C6})(12) - \delta(\text{O10O11C6})(9) - (\omega-\text{CH2})(8) - \nu(\text{N1C2})(6)$
83	1235	1187	1.74	1187	$\nu(\text{C22C25})(43) - (\delta\text{trigonal-R1})(13) - \delta(\text{C22H42C23})(7) - \nu(\text{C21C22})(7) \delta(\text{C20H41C21})(7) - \nu(\text{C22C23})(6) - \nu(\text{C20C21})(5) - \nu(\text{C23C24})(5)$
82	1213	1165	4.67		$\delta(\text{C22H27N1})(34) \nu(\text{N1C2})(20) (\rho-\text{Me3})(5)$
81	1211	1163	4.99	1156	$\delta(\text{C20H41C21})(20) - \delta(\text{C19H40C20})(18) - (\omega-\text{C24H43})(17) - \delta(\text{C22H42C23})(17) \nu(\text{C20C21})(10) \nu(\text{C23C24})(9)$
80	1185	1138	3.96		$(\rho-\text{CH2})(51) (\rho-\text{Me1})(36) - (\text{t-CH2})(6) (\delta\text{as-Me1})(4) - 5\nu(\text{N1H27})(1)$
79	1143	1098	61.95	1092	$(\rho-\text{Me1})(17) - \nu(\text{C12C13})(10) - \nu(\text{S16O18})(10) - \nu(\text{S16O17})(8) - \nu(\text{C6O11})(8) - (\delta\text{sc-C12O11C13})(8) \nu(\text{S16C19})(6)$
78	1142	1098	137.9		$\nu(\text{S16O17})(14) \nu(\text{S16O18})(13) - \nu(\text{S16C19})(12) (\rho-\text{Me1})(10) \nu(\text{C19C24})(6) - \nu(\text{C12C13})(5) \delta(\text{C19H40C20})(5) (\delta\text{as-Me1})(5)$
77	1142	1097	12.4		$(\omega-\text{C24H43})(18) \nu(\text{C20C21})(15) \delta(\text{C20H41C21})(14) \delta(\text{C22H42C23})(14) - \nu(\text{C23C24})(13) - \delta(\text{C19H40C20})(12)$
76	1134	1089	179.13	1018	$\nu(\text{O11C12})(17) - (\rho-\text{Me1})(12) - \nu(\text{C6O11})(10) (\delta\text{R})(9) \nu(\text{C3C9})(8) - \delta(\text{N14C4C8})(5) \nu(\text{N14N15})(5)$
75	1106	1063	7.89		$\nu(\text{N14N15})(35) (\rho-\text{Me3})(12) - \delta(\text{N14C4C8})(7) - (\rho-\text{Me4})(5)$
74	1090	1047	34.39		$(\rho-\text{Me4})(28) - \delta(\text{R})(12) \nu(\text{C5C7})(7) \delta(\text{N14C26C8})(7) (\rho-\text{Me3})(7) \nu(\text{C4C5})(6) \delta(\text{R})(5)$
73	1086	1043	150.1		$\nu(\text{S16O18})(20) \nu(\text{S16O17})(17) - (\delta\text{as-Me1})(11) \nu(\text{C19C24})(11) \nu(\text{N14N15})(5)$
72	1065	1024	13.02		$(\rho-\text{Me5})(48) (\rho-\text{Me5})(15) (\delta\text{oop-C22C25})(10) - (\text{R1-puckering})(7) (\delta\text{as-Me5})(5) - (\omega-\text{C24H43})(5) - (\omega-\text{C21H41})(5)$

(continued on next page)

Table 5b (continued)

Mode no.	V Unsc.	V Scal,	Intensity	V Exp.	Assignment (PED) $\geq 5\%$
71	1064	1022	6.77		(p-Me3)(68)(oop-C3C9)(7)(t-R)(6)
70	1059	1017	6.47		(p-Me2)(42)(p-Me2)(10)(p-Me4)(9)-oop-C5C6)(6)(as-Me2)(5)
69	1053	1012	1.62		(p-Me4)(21)-(p-Me2)(17)(p-Me3)(11)-δ(C8C26)(7)-(p-Me2)(6)-v(N14N15)(6)
68	1049	1008	48.87	953	v(C12C13)(42)-v(O11C12)(31)
66	1033	992.4	6.35		(δtrigonal-R1)(62)-v(C22C23)(9)-v(C21C22)(8)v(S16C19)(3)(as-Me1)(2)
64	1007	967.6	2.81		(p-Me2)(36)-(p-Me2)(16)(p-Me3)(11)-v(N1C5)(10)δ(R)(5)(as-Me2)(5)
63	982	943.9	18.54		v(C8C26)(36)(p-Me4)(16)v(N14N15)(10)-δ(N15H39N14)(8)v(C8N14)(6)
62	979	940.6	0.46		(ω-C20H40)(30)-(ω-C21H41)(28)(ω-C24H43)(17)(ω-C24H43)(16)(t-R1)(8)
61	972	933.9	0.74		(ω-C24H43)(31)(ω-C24H43)(22)-(ω-C20H40)(18)(R1-puckering)(14)(ω-C21H41)(11)
60	906	870	31.41	836	v(O11C12)(23)(p-Me1)(13)v(C12C13)(12)v(N15S16)(6)-δ(N15H39N14)(5)
59	897	862.1	278.97	815	v(N15S16)(22)-δ(N15H39N14)(13)-v(O11C12)(9)-v(N14N15)(8)-(p-N15N14S16)(8)-(p-Me4)(7)(δ-C8N14N15)(7)-(p-Me1)(5)
58	864	830	25.67		δ(O10011C6)(17)v(C6O11)(16)-δ(C12C6O11)(14)(p-Me1)(11)v(C2C3)(5)
56	828	796	18.25	793	(ω-C21H41)(20)(ω-C24H43)(20)-(ω-C24H43)(18)(ω-C20H40)(17)-(t-R1)(8)
53	768	737.7	17.95	774	δ(R)(27)δ(O10011C6)(17)v(C5C7)(16)-v(C3C9)(12)-δ(C3C8C4)(5)
52	754	724	15.76	741	(oop-C2C6)(48)(oop-C2C6)(17)(t-C6C2)(16)(t-R)(8)
51	720	691.7	9.76		(t-R)(34)-(oop-C4C8)(22)-(oop-C5C6)(9)-(t-C4C8)(8)(oop-C3C9)(7)(t-R)(5)
50	718	689.4	79.72	685	(R1-puckering)(52)-(oop-C16C19)(7)-(oop-C22C25)(7)
49	708	679.9	50.04		(R1-puckering)(48)-(oop-C22C25)(6)v(C8C26)(5)
48	653	627	56.84		v(S16C19)(10)-δ(N1C6C2)(7)-δ(C2C9C3)(7)(ω-SO2)(6)-δ(C3C8C4)(5)-v(C22C25)(5)
47	650	624.5	19.5	615	(ω-N1H27)(53)-(oop-C3C9)(11)-(t-R)(10)
45	636	611.3	11.04		v(S16C19)(10)-(ω-N15H39)(10)δ(C8C26)(7)(as-R1)(6)δ(C3C8C4)(6)-v(C22C25)(5)δ(N1C6C2)(5)
44	614	589.9	50.16		(ω-N1H27)(39)(t-R)(36)(oop-C2C6)(7)-(oop-C5C6)(5)
43	598	574.4	90.67		(ω-N15H39)(35)(p-N15N14S16)(17)v(N15S16)(12)
42	581	558.3	11.95	553	(ω-N1H27)(25)(p-N15N14S16)(11)δ(R)(10)-v(C5C7)(7)-v(C3C9)(7)
41	558	535.8	36.34		δ(C8C26)(26)-(ω-N15H39)(7)-(p-N15N14S16)(6)(t-C4C8)(5)
40	537	515.9	85.12		(ω-SO2)(19)δ(C8C26)(11)-(as-R1)(10)(ω-N15H39)(8)(sc-SO2)(6)-(t-R1)(5)
39	510	490.1	30.66		(ω-N15H39)(22)(p-N15N14S16)(12)-(t-R1)(12)(oop-C16C19)(6)-(oop-C22C25)(6)-(sc-SO2)(6)δ(N15H39N14)(5)
38	496	476.5	14.89	483	(ω-N15H39)(27)(p-N15N14S16)(18)(p-SO2)(14)δ(C8C26)(8)
37	479	460	10.01	469	(t-R1)(23)-(sc-SO2)(14)(oop-C22C25)(14)-(oop-C16C19)(9)-δ(N1C7C5)(5)

Proposed assignment and potential energy distribution (PED) for vibrational modes: types of vibrations: v – stretching, δsc – scissoring, p – rocking, ω – wagging, t – twisting, δ – deformation, δs – symmetric deformation, δas – asymmetric deformation, δip – in plane deformation, δoop – out of plane deformation, τ – torsion, R – pyrrole ring, R₁ phenyl ring, Me, Me1, Me2, Me3, Me4, Me5 – methylgroup.

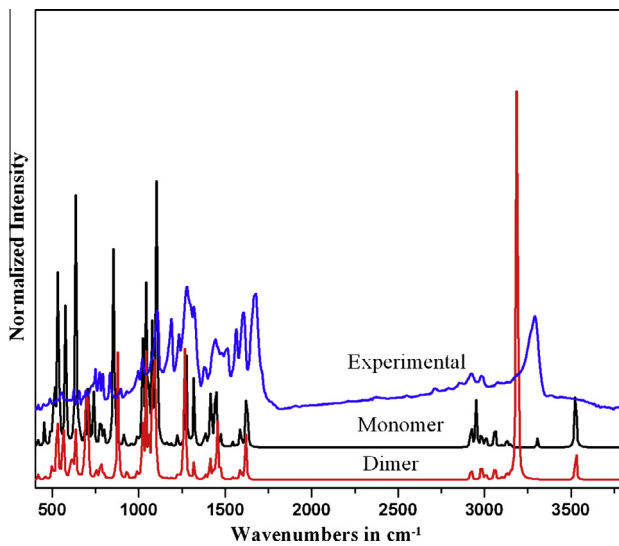


Fig. 6a. Comparison between experimental and theoretical IR spectrum for PT. correspond to the earlier reported absorption band at 1440, 800–700 cm⁻¹ in the region [40].

C=O Vibrations

The carbonyl stretching vibration is highly characteristic and intense absorption. The stretching vibration of ester carbonyl group ($\nu_{C=O}$) in EDTEPC observed at 1665 cm⁻¹ corroborates well with calculated wavenumber at 1690 cm⁻¹. The observed $\nu_{C=O}$ at 1665 cm⁻¹ also corresponds to the earlier reported wavenumber at 1665 cm⁻¹ for dimer of our previous studies of hydrazones [35–37]. Therefore, stretching mode of $\nu_{C=O}$ in EDTEPC confirms

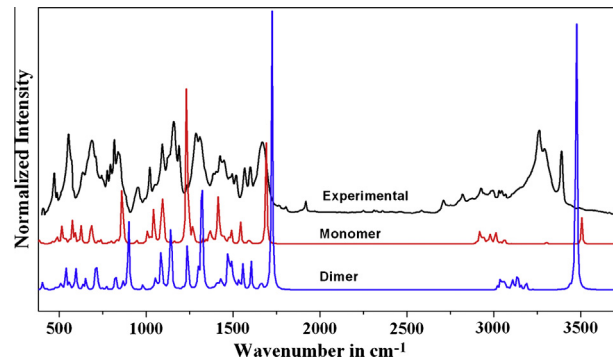


Fig. 6b. Comparison between experimental and theoretical IR spectrum for EDTEPC.

the involvement of C=O group in intermolecular hydrogen bonding. The red shift in the stretching wavenumber of hydrogen bond acceptor (C=O) has been clearly observed in the experimental and theoretical spectrum due to its hydrogen bond free C=O group in monomer. The ester C=O stretching ($\nu_{C=O-C}$) observed in EDTEPC at 1092 cm⁻¹ and calculated and these bands occur in the region 1300–1000 cm⁻¹ in literature [40].

C=C vibrations

In aromatic hydrocarbons, the skeletal vibrations involving carbon–carbon stretching within the ring absorb in the 1600–1585 cm⁻¹ and 1500–1400 cm⁻¹ region and out-of-plane bending vibrations in substituted benzenes absorb near 694–558 cm⁻¹ [40]. The C=C stretches in EDTEPC of pyrrole is assigned at 1492 cm⁻¹, in FT-IR spectrum and also along with the reported band in literature in the region 1420–1360 cm⁻¹ [39]. The observed

Table 6

Calculated $\varepsilon_{\text{HOMO}}$, $\varepsilon_{\text{LUMO}}$, energy band gap ($\varepsilon_{\text{L}} - \varepsilon_{\text{H}}$), chemical potential (μ), electronegativity (χ), global hardness (η), global softness (S), global electrophilicity index (ω) for (1), (2), (3), (5), (6) and Electrophilicity based charge transfer (ECT) for reactant system [(1) \leftrightarrow (2)] and [(5) \leftrightarrow (2)] of PT and EDTEPC.

	ε_{H}	ε_{L}	$\varepsilon_{\text{H}} - \varepsilon_{\text{L}}$	χ	μ	η	S	ω	ECT
<i>PT</i>									
(1)	-6.2641	-1.257	5.0071	3.7605	-3.7605	2.5035	0.1997	2.8243	0.219
(2)	-6.9128	-0.8561	6.0568	3.8845	-3.8845	3.0284	0.1651	2.4913	
(3)	-5.7370	-1.118	4.619	3.4275	-3.4275	2.3095	0.2164	2.5433	
<i>EDTEPC</i>									
(5)	-6.0315	-0.8158	5.2157	3.4237	-3.4237	2.6079	0.1917	2.2473	
(2)	-6.9128	-0.8561	6.0568	3.8845	-3.8845	3.0284	0.1651	2.4913	0.030
(6)	-5.6491	-0.9252	4.7239	3.2872	-3.2872	2.362	0.2116	2.2874	

ε_{H} , ε_{L} , $\varepsilon_{\text{L}} - \varepsilon_{\text{H}}$, χ , μ , η , ω (in eV) and S (in eV^{-1}).

Table 7

Selected electrophilic reactivity descriptors (f_k^+ , s_k^+ , ω_k^+) for reactant (1, 5) and nucleophilic reactivity descriptors (f_k^- , s_k^- , ω_k^-) for reactant (2), using Hirshfeld atomic charges of PT and EDTEPC.

Sites	f_k^+	s_k^+	ω_k^+	Sites	f_k^-	s_k^-	ω_k^-
<i>PT</i>							
C2	0.0644	0.0025	0.5665	N1	0.1433	0.0240	0.4135
C3	0.0098	0.0003	0.0866	N20	0.1566	0.0263	0.4516
C4	0.1633	0.0065	1.4348				
C6	0.1402	0.0056	1.2323				
<i>EDTEPC</i>							
7 C	0.0143	0.0169	0.0321	N1	0.1433	0.0240	0.4135
15 C	0.0078	0.2761	0.0175	N20	0.1566	0.0263	0.4516

f_k , f_k^- (in e); s_k^+ , s_k^- (in eV^{-1}) and ω_k^+ , ω_k^- (in eV).

Table 8

Calculated Dipole moment (μ_0), Polarizability ($|\alpha_0|$), anisotropy of Polarizability ($\Delta\alpha$), First Hyperpolarizability (β_0) and their components, using B3LYP/6-31G(d,p) of PT and EDTEPC.

Dipole moment		Polarizability		Hyperpolarizability	
PT	EDTEPC	PT	EDTEPC	PT	EDTEPC
μ_x	0.3043	1.990	α_{xx}	218.298	328.19
μ_y	2.2395	3.492	α_{yy}	22.132	7.423
μ_z	-0.7493	-2.195	α_{zz}	173.263	221.57
μ_0	2.1322	4.5797	$ \alpha_0 $	137.89	27.5248
			$\Delta\alpha$	94.1024	β_{xxx}
					-929.20
					959.48
					β_{xyy}
					61.37
					245.51
					β_{yyx}
					-43.59
					99.826
					β_{xxy}
					-31.48
					-88.448
					β_{yyz}
					-93.05
					-211.86
					β_{xyz}
					-91.12
					-85.242
					β_{yyz}
					-31.39
					-22.051
					β_{xzz}
					-30.21
					-129.11
					β_{yzz}
					28.74
					1.110
					β_{zzz}
					-80.34
					7.162
					β_0
					6.509
					8.3837

μ_0 in Debye; $|\alpha_0|$ and $\Delta\alpha$ in 10^{-24} esu; β_0 in 10^{-30} esu.

C—C—C deformations associated with pyrrole ring at 896, 793 cm^{-1} in PT and EDTEPC, respectively. In theoretical IR spectrum, the combination bands of 'C—C stretches and C—C—H deformations' associated with benzene ring are observed at 1451, 1420 cm^{-1} . The C=C stretches of benzene is observed at 1566 cm^{-1} in EDTEPC. The observed C=C stretches of benzene at 1565 cm^{-1} also corresponds well with the calculated wavenumber at 1543 cm^{-1} [40].

S=O vibrations, S—N vibrations

The asymmetric and symmetric stretching vibrations of SO_2 ($\nu_{\text{S=O}}$) in PT and EDTEPC are observed at 1233, 1108, 1232, 1156 cm^{-1} , correlate well with the theoretical wavenumber at 1227, 1102, 1233, 1163 cm^{-1} , respectively. Thus, red shift in the observed wavenumbers indicates the involvement of SO_2 group in hydrogen bonding in the solid state. The free asymmetric and symmetric $\nu_{\text{S=O}}$ is also reported in the literature at 1360, 1168 cm^{-1} for sulfonamide triazines [41].

C=N vibrations

The observed C=N stretching vibration ($\nu_{\text{C=N}}$) in PT and EDTEPC at 1588, 1597 cm^{-1} , matches well with the theoretically calculated wavenumber at 1589, 1600 cm^{-1} , respectively. The observed $\nu_{\text{C=N}}$ at 1588, 1598 cm^{-1} also corresponds to the earlier reported wavenumber at 1602 cm^{-1} [40]. In FT-IR spectrum of PT, the presence of C=N band confirms the formation of hydrazone linkage in the molecules.

Global and local reactivity descriptors analysis

The chemical reactivity and site selectivity of the molecular systems have been determined on the basis of Koopman's theorem [42]. Global reactivity descriptors as electronegativity (χ) = $-1/2(\varepsilon_{\text{LUMO}} + \varepsilon_{\text{HOMO}})$, chemical potential (μ) = $1/2(\varepsilon_{\text{LUMO}} + \varepsilon_{\text{HOMO}})$, global hardness (η) = $1/2(\varepsilon_{\text{LUMO}} - \varepsilon_{\text{HOMO}})$, global softness (S) = $1/2\eta$ and electrophilicity index (ω) = $\mu^2/2\eta$ are highly successful in predicting global reactivity trends [43–46]. The energies of frontier molecular orbitals ($\varepsilon_{\text{HOMO}}$, $\varepsilon_{\text{LUMO}}$), energy gap ($\varepsilon_{\text{HOMO}} - \varepsilon_{\text{LUMO}}$), electronegativity (χ), chemical potential (μ), global hardness (η), global softness (S), global electrophilicity index (ω) for (1), (2), (3) and ECT for reactant system [(1) \leftrightarrow (2)] and [(5) \leftrightarrow (2)] are listed in Table 6. The global electrophilicity index (ω = 2.54, 2.287 eV) of PT and EDTEPC show these molecule behaves as a strong electrophile.

Electrophilic charge transfer (ECT) = $(\Delta N_{\text{max}})_A - (\Delta N_{\text{max}})_B$ is defined as the difference between the ΔN_{max} values of interacting molecules [46]. If we consider two molecules A and B approach to each other (i) if ECT > 0, charge flow from B to A (ii) if ECT < 0, charge flow from A to B. ECT is calculated as 0.219, 0.030 for reactant molecules [(1), (2)], [(5) and (2)], which indicates that charge flows from (2) to (1) and (2) to (5). Therefore, (1 and 5) acts as electron acceptor (electrophile) and (2) as electron donor (nucleophile). Selected local electrophilic reactivity descriptors (f_k^+ , s_k^+ , ω_k^+) [43–47], for reactant (1), (5) and nucleophilic reactivity descriptors (f_k^- , s_k^- , ω_k^-) for reactant (2) are given in Table 7. Using Hirshfeld charges, the maximum values of local electrophilic reactivity descriptors (f_k^* , s_k^* , ω_k^*) at aldehyde carbon C6, C7 of reactants (1) and (5) indicate that these are the most electrophilic site in the studied molecules. The nucleophilic reactivity descriptors (f_k^- , s_k^- , ω_k^-) analysis of reactant (2) shows that N20 is the most nucleophilic site. Therefore, the nucleophilic attack of N20 site of reactant (2) at the most electrophilic site C6, C7 of reactants (1) and (2) confirm the formation of product molecule (3) and (6) or Schiff base linkage (C=N) in hydrazone.

Static dipole moment (μ_0), mean polarizability ($|\alpha_0|$), anisotropy of polarizability ($\Delta\alpha$) and first hyperpolarizability (β_0)

In order to investigate the relationship between molecular structure and NLO response, first hyperpolarizability (β_0) of this novel molecular system, and related properties ($|\alpha_0|$ and $\Delta\alpha$) are

calculated using B3LYP/6-31G(d,p), based on the finite-field approach and their calculated values are given in Table 8. As we know hyperpolarizability is difficult task to measure directly, computational calculation is an alternate choice and provides another method to investigate extensive properties of materials. Large value of particular component of the polarizability and hyperpolarizability indicate a substantial delocalization of charge in these directions. Since the value of the polarizability ($|\alpha_0|$), first hyperpolarizability (β_0) of Gaussian 09 output are reported in atomic unit (a.u.) and these values are converted into electrostatic unit (esu) using converting factors as (for α_0 : 1 a.u. = 0.1482×10^{-24} esu; for β_0 : 1 a.u. = 0.008639×10^{-30} esu). The first hyperpolarizability (β_0) of the PT and EDTEPC are calculated as 6.509×10^{-30} , 8.383×10^{-30} esu, respectively. In this study, *p*-Nitroaniline (*p*-NA, $\beta_0 = 11.54 \times 10^{-30}$ esu) is chosen as a reference molecule because there were no experimental values for PT and EDTEPC. Therefore, investigated molecule will show non-linear optical response and might be used as non-linear optical (NLO) material.

Conclusions

The synthesized pyrrole tosylhydrazones have been carried out using various spectroscopic techniques (Mass, ^1H NMR, UV-Visible, FT-IR). TD-DFT is used to find various electronic excitations and their nature within molecule. The red shift in both the proton donor (pyrrole N—H) and proton acceptor (S=O) group designates presence of intermolecular classical hydrogen bonding N—H···O in PT molecule. In EDTEPC dimer, the stretching wavenumber of hydrogen bond donor (N—H) is red-shifted due to the elongation of hydrogen bond donor (N—H bond) than the hydrogen bond free N—H group in monomer. The calculated binding energy of EDTEPC and PT dimer formation are found as 13.12, 14.12 kcal/mol, respectively, after correction in basis set superposition error (BSSE) via standard counterpoise method. The local reactivity descriptors analyses are performed to determine the reactive sites within molecule. First hyperpolarizability (β_0) of EDTEPC and PT is computed to evaluate non-linear optical (NLO) response of the investigated molecule.

Acknowledgement

The authors are thankful to the DST New Delhi for financial supports.

Appendix A. Supplementary material

Supplementary data associated with this article can be found, in the online version, at <http://dx.doi.org/10.1016/j.molstruc.2014.10.046>.

References

- [1] N.P. Belskaya, W. Dehaen, V.A. Bakuleva, ARKIVOC i (2010) 275–332.
- [2] Ü.O. Özdemir, P. Güvenç, E. Sahin, F. Hamurcu, Inorg. Chim. Acta 362 (2009) 2613–2618.
- [3] B. Kalluraya, A.M. Isloor, P.V. Frank, R.L. Jagadeesha, Ind. J. Het. Chem. 13 (2004) 245–248.
- [4] K.N. de Oliveira, P. Costa, J.R. Santin, L. Mazzambani, C. Bürger, C. Mora, R.J. Nunes, Bioorg. Med. Chem. 19 (2011) 4295–4306.
- [5] S.M. Sondhi, M. Dinodia, A. Kumar, Bioorg. Med. Chem. 14 (2006) 4657–4663.
- [6] A.C. Cunha, J.L.M. Tributino, A.L.P. Miranda, C.A.M. Fraga, E.J. Barreiro, IL Fármaco 57 (2002) 999–1012.
- [7] S.K. Sridar, A. Ramesh, Biol. Pharm. Bull. 24 (2001) 1149–1152.
- [8] S. Siemann, D.P. Evanoff, L. Marrone, A.J. Clarke, T. Viswanatha, G.I. Dmitrienko, Antimicrob. Agents Chemother. 46 (2002) 2450–2457.
- [9] F.I. Raynaud, P. Parker, P. Workman, M.D. Waterfield, Bioorg. Med. Chem. 15 (2007) 5837–5844.
- [10] R.A. Jones, G.P. Bean, The Chemistry of Pyrroles, Academic Press, London, 1977. pp. 525.
- [11] S.J. Hong, M.H. Lee, C.H. Lee, Bull. Korean Chem. Soc. 25 (2004) 1545–1550.
- [12] R.T. Hayes, M.R. Wasilewski, D. Gosztola, J. Am. Chem. Soc. 122 (2000) 5563–5567.
- [13] M. Harmjanz, H.S. Gill, M.J. Scott, J. Am. Chem. Soc. 122 (2000) 10476–10477.
- [14] A. Sour, M.L. Boillot, E. Riviere, P. Lesot, Eur. J. Inorg. Chem. 1999 (1999) 2117–2119.
- [15] S. Scheiner, Y. Gu, T. Kar, J. Mol. Struct.: Theochem. 500 (2000) 441–452.
- [16] F.H. Allen, V.J. Hoy, J.A.K. Howard, V.R. Thalladi, G.R. Desiraju, C.C. Wilson, G.J. McIntyre, J. Am. Chem. Soc. 119 (1997) 3477–3480.
- [17] L. Zhou, F. Ye, Y. Zhang, J. Wang, J. Am. Chem. Soc. 132 (2010) 13590–13591.
- [18] X. Zhao, J. Jing, K. Lu, Y. Zhang, J. Wang, Chem. Commun. 46 (2010) 1724–1726.
- [19] A.K. Tyrlík, S. Marczałk, K. Michałak, J. Wicha, A. Zarecki, J. Org. Chem. 66 (2001) 6994–7001. confirms.
- [20] S. Zhu, Y. Liao, S. Zhu, Org. Lett. 6 (2004) 377–380.
- [21] L. Zhou, Y. Shi, Q. Xiao, Y. Liu, F. Ye, Y. Zhang, J. Wang, Org. Lett. 13 (2011) 968–971.
- [22] J.S. Ghomi, J. Chin. Chem. Soc. 54 (2007) 1561–1563.
- [23] A. Reguig, M.M. Mostafa, L. Larabi, Y. Harek, J. App. Sci. 8 (2008) 3191–3198.
- [24] R. Juneau, S. Mitchell, G. Wolgamott, J. Pharm. Sci. 68 (1978) 930–931.
- [25] P. Rawat, R.N. Singh, J. Mol. Struct. 1074 (2014) 201–212.
- [26] P. Rawat, R.N. Singh, J. Mol. Struct. 1075 (2014) 462–470.
- [27] C.F. Matta, J.H. Trujillo, T.H. Tang, R.F.W. Bader, Chem. Eur. J. 9 (2003) 1940–1951.
- [28] M.J. Frisch, G.W. Trucks, H.B. Schlegel, G.E. Scuseria, M.A. Robb, J.R. Cheeseman, G. Scalmani, V. Barone, B. Mennucci, G.A. Petersson, H. Nakatsuji, M. Caricato, X. Li, H.P. Hratchian, A.F. Izmaylov, J. Bloino, G. Zheng, J.L. Sonnenberg, M. Hada, M. Ehara, K. Toyota, R. Fukuda, J. Hasegawa, M. Ishida, T. Nakajima, Y. Honda, O. Kitao, H. Nakai, T. Vreven, J.A. Montgomery, Jr., J.E. Peralta, F. Ogliaro, M. Bearpark, J.J. Heyd, E. Brothers, K.N. Kudin, V.N. Staroverov, T. Keith, R. Kobayashi, J. Normand, K. Raghavachari, A. Rendell, J.C. Burant, S.S. Iyengar, J. Tomasi, M. Cossi, N. Rega, J.M. Millam, M. Klene, J.E. Knox, J.B. Cross, V. Bakken, C. Adamo, J. Jaramillo, R. Gomperts, R.E. Stratmann, O. Yazyev, A.J. Austin, R. Cammi, C. Pomelli, J.W. Ochterski, R.L. Martin, K. Morokuma, V.G. Zakrzewski, G.A. Voth, P. Salvador, J.J. Dannenberg, S. Dapprich, A.D. Daniels, O. Farkas, J.B. Foresman, J.V. Ortiz, J. Cioslowski, D.J. Fox, Gaussian 09, Revision B.01, Gaussian Inc., Wallingford, CT, 2010.
- [29] J.M.L. Martin, V. Alsenoy, C.V. Alsenoy, Gar2ped software, University of Antwerp, 1995.
- [30] Todd A. Keith, TK Grismill Software, Overland Park KS, USA, 2010 AIMAll (Version 10.06.21) <aim.tkggristmill.com>.
- [31] W.H. Ojala, W.B. Gleason, Acta. Cryst. C54 (1998) 63–66.
- [32] S.F. Boys, F. Bernardi, Mol. Phys. 19 (1970) 553–556.
- [33] J.P. Merrick, D. Moran, L. Radom, J. Phys. Chem. A 111 (2007) 11683–11700.
- [34] A.T. Dubis, S.J. Grabowski, D.B. Romanowska, T. Misiaszek, J. Leszczynski, J. Phys. Chem. A 106 (2002) 10613–10621.
- [35] R.N. Singh, A. Kumar, P. Rawat, A. Srivastava, J. Mol. Struct. 1049 (2014) 419–428.
- [36] R.N. Singh, P. Rawat, S. Sahu, J. Mol. Struct. 1054–1055 (2013) 123–133.
- [37] R.N. Singh, P. Rawat, J. Mol. Struct. 1054–1055 (2013) 65–75.
- [38] P. Pulay, G. Fogarosi, F. Pang, J.E. Boggs, J. Am. Chem. Soc. 101 (1979) 2550–2560.
- [39] D.L. Pavia, G.M. Lampman, G.S. Kriz, Introduction to spectroscopy, Ed. 3 (2001)
- [40] R.M. Silverstein, F.X. Webster, Spectrometric Identification of Organic Compounds, 6th ed., Jon Wiley Sons Inc., New York, 1963. pp. 215–274.
- [41] H.A. Dabbagh, A. Teimouri, R. Shiasi, A.N. Chermahini, J. Iran. Chem. Soc. 5 (2008) 74–82.
- [42] R.G. Parr, W. Yang, Density Functional Theory of Atoms and Molecules, Oxford University Press, Oxford, New York, 1989. pp. 215–274.
- [43] R.N. Singh, P. Rawat, S. Sahu, J. Mol. Struct. 1065 (2014) 99–107.
- [44] R.N. Singh, V. Baboo, P. Rawat, V.P. Gupta, J. Mol. Struct. 1037 (2013) 338–351.
- [45] R.N. Singh, V. Baboo, P. Rawat, A. Kumar, D. Verma, J. Mol. Struct. 94 (2012) 288–301.
- [46] R.N. Singh, A. Kumar, R.K. Tiwari, P. Rawat, J. Mol. Struct. 1035 (2013) 295–306.
- [47] P. Rawat, R.N. Singh, J. Mol. Struct. 1074 (2013) 201–212.